



UNIVERSITY OF NAIROBI

**EXPLORING THE EVIDENCE FOR A CLOSED UNIVERSE: IS THERE
A POSSIBLE CRISIS FOR COSMOLOGY?**

BY

DOUGLAS OMURWA MANASI

I56/34466/2019

**A Research Project Submitted in Partial Fulfillment of the Requirements
for Award for the Degree of Master of Science in Physics (Astrophysics) of
the University of Nairobi**

2021

DECLARATION

I declare that this project is my original work and has not been submitted elsewhere for examination, award of a degree or publication. Where other people's work or my own work has been used, this has properly been acknowledged and referenced in accordance with the University of Nairobi's requirements.

Signature.......... Date..22/07/2021

DOUGLAS OMURWA MANASI

I56/34466/2019

Department of Physics

School of Physical Sciences

University of Nairobi

This thesis is submitted for examination with our approval as research supervisors:

Signature

Date

Dr. Geoffrey O. Okeng'o

..........

22/07/2021

Department of Physics

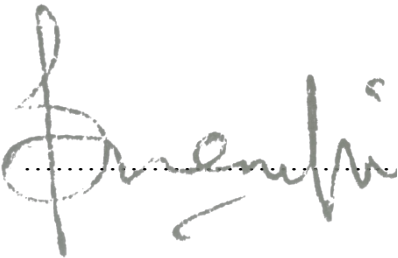
University of Nairobi

P.O Box 30197-00100

Nairobi Kenya

gokengo@uonbi.ac.ke

Dr. John B. Awuor

..........

22/07/2021

Department of Physics

University of Nairobi

P.O Box 30197-00100

Nairobi Kenya

buers@uonbi.ac.ke

DEDICATION

I dedicate this research work to my family members, my father Samuel Manasi Sangia and my mother Jane Moraa Manasi, my brothers Edwin Nyakundi, Brian Nyakoni and Duncan Mosioma, my sisters Sabinah, Alice, Lilian, Jackline and Teresiah and all my friends for their advice, encouragement and support during my studies.

ACKNOWLEDGEMENT

The success of this project was made possible by the guidance and support of many people. My kind appreciation goes to the administration of the University of Nairobi and the Department of physics for the support, provision of adequate resources and guidance which contributed greatly to the success of this thesis. My sincere thanks go to Prof Leonidah Kerubo, dean, Chiromo campus for the support and guidance whenever needed. My sincere gratitude to my supervisors Dr. Geoffrey O. Okeng'o and Dr. John B. Awuor who were always available to answer my questions and made sure my equations were accurate. I am grateful to Prof Charles Ondieki from Multimedia University and Mr. Raymond Samuel Machogu for their financial support and advice. Special thanks to Mr. Edwin Nyakundi Manasi for the accommodation during my research. I thank God for the gift of life and good health during this project.

ABSTRACT

This research project aims at exploring the validity of the recently published work by Di Valentine *et al.* (2019) which used the Planck Legacy 2018 (PL18) data that suggested a possibility of a closed universe in which the amplitude of Cosmic Microwave Background radiations is enhanced and prefers a positive curvature at 99% cadence level. The study by Di Valentino *et al.* (2019) is based on the observations of the ancient light called Cosmic Microwave Background (CMB). In the report, the amplitude of the CMB is larger compared to that of the standard Λ CDM model and the data deviates by 3.4 standard deviations. This research work investigates this amplitude abnormality, derive equations governing dynamics of a closed Universe within Einstein General Relativity, and develop relevant theory behind possible crisis with regard to the proposed evidence of a closed universe by considering the Friedmann-Robertson-Walker (FRW) metric which assumes a homogeneous and an isotropic universe. We analyze the implications of a closed universe in cosmology. This research work begins by deriving the first and second Friedmann equations using the Einstein Field Equations (EFE). Then the continuity equation is derived by considering a perfect fluid. Three coupled differential equations for Hubble parameter, scale factor and density as functions of time are obtained and transformed to two coupled differential equations of Hubble parameter and density parameter as functions of scale factor. The two equations are solved simultaneously using Python – Spyder package called Odeint and plotted graphs of evolution of Hubble parameter and density parameter for Einstein de Sitter (EdS) model, the standard Λ CDM model and compared to that of closed universe. From the graphs obtained, the Hubble parameter decreases with increase in the scale factor. The value of Hubble parameter in EdS at decoupling is greater than that of Λ CDM and closed models but their values converge today. The density parameter for a closed universe is greater than one compared to that Einstein de Sitter model and Λ CDM values which is one. This implies that the closed cosmos has enough matter to cause a deceleration in its expansion. The deceleration implies that at some time in future the expansion will stop and big crunch will occur. If indeed the universe is closed, then the current cosmology is in a crisis. Since the Planck spectra from Planck’s Legacy 2018 prefers a closed universe, however, the anomalies might have risen from undetected systematics and/or statistical fluctuations, this study recommends that more observations to be carried out to ascertain whether there is a possible paradigm shift in cosmology and new physics is required.

TABLE OF CONTENTS

DECLARATION	i
DEDICATION.....	ii
ACKNOWLEDGEMENT	iii
ABSTRACT.....	iv
LIST OF TABLES	vii
LIST OF FIGURES	viii
LIST OF ABBREVIATIONS/ACRONYMS AND SYMBOLS.....	ix
CHAPTER ONE: INTRODUCTION.....	1
1.1 Research Background	1
1.1.1 Geometry of our Universe	1
1.1.2 The Cosmic Microwave Background	3
1.1.3 Standard cosmological model	4
1.2 Theory: History of cosmology	4
1.3 Statement of the Problem.....	8
1.4 Objectives	8
1.4.1 Main Objective.....	8
1.4.2 Specific Objectives.....	8
1.5 Justification and Significance of the Study.....	9
CHAPTER TWO: LITERATURE REVIEW.....	10
CHAPTER THREE: THEORETICAL FRAMEWORK.....	23
3.1 Einstein Field Equations	23
3.2 Friedman–Lemaitre–Robertson–Walker (FLRW) Metric.....	23
3.3 Density and Density parameter	26
3.4 Cosmic Microwave Background (CMB) Radiation.....	27
CHAPTER FOUR: RESEARCH METHODOLOGY	29
4.1.1 Source of Data.....	29
4.1.2 Planck, WMAP.....	29
4.1.3 Data type and Description.....	29
4.1.4 Data Analysis Tools	30
4.2 The Governing Equations	30
4.2.1 Einstein Field Equations	30
4.2.2 Energy-Momentum Conservation	44
4.2.3 Matter density And Density Parameter.....	47
4.2.4 Dynamical Equations.....	51
CHAPTER FIVE: RESULTS AND DISCUSSION.....	56

CHAPTER SIX: CONCLUSION AND RECOMMENDATION	61
References	62

LIST OF TABLES

Table 2. 1: Tensions between PL18 and BAO and CMB Lensing.

18

LIST OF FIGURES

Figure 2. 1: Preference for a closed universe (Di Valentino E, 2019).....	14
Figure 2. 2: Degeneracy between curvature and lensing (Di Valentino E, 2019).....	16
Figure 2. 3: Curvature and parameters shift (Di Valentino E, 2019).....	16
Figure 2. 4: Tension with CMB lensing (Di Valentino E, 2019).....	18
Figure 2. 5: Tension with cosmic shear measurements (Di Valentino E, 2019).....	19
Figure 2. 6: Tension with combined data (Di Valentino E, 2019).....	20
Figure 2. 7: Tensions in combined data (Di Valentino E, 2019).....	20
Figure 6. 1: A graph of h as a function of the scale factor	56
Figure 6. 2: A graph of a density parameter against scale factor.....	56
Figure 6. 3: A graph of h as a function of the scale factor for Λ CDM model.....	57
Figure 6. 4: A graph of density parameter for Λ CDM against the scale factor.....	57
Figure 6. 5: A graph of h against scale factor (a) in closed model.....	58
Figure 6. 6: A graph of density parameter with respect to scale factor for a closed universe	58
Figure 6. 7: Comparing the graphs of dimensionless Hubble parameter in EdS, Λ CDM and closed models.....	59
Figure 6. 8: Comparing the graphs of density parameter as a function of the scale factor in EdS, Λ CDM and closed models	59

LIST OF ABBREVIATIONS/ACRONYMS AND SYMBOLS

FLRW	Friedman-Lemaitre-Robertson-Walker
CP	Copernican Principle
BAO	Baryon acoustic oscillation
SKA	Square Kilometer Array
CMB	Cosmic Microwave Background Radiation
OHD	Observational Hubble parameter data
SDSS	Sloan Digital Sky Survey
Mpc	mega parsecs
H	Planck's constant
Kpc	kilo parsecs
WMAP	Wilkinson Microwave Anisotropy Probe
LAMBDA	Legacy Archive for Microwave Background Data Analysis
NASA	National Aeronautics and Space Administration
FWHM	Full Width Half Maximum
EFE	Einstein Field Equations
DM	Dark matter
PL	Planck's Legacy
EoS (w)	Equation of state

CHAPTER ONE: INTRODUCTION

1.1 Research Background

Cosmology is a discipline in astronomy that studies the universe as a whole with an assumption that at the largest scales the universe obeys the homogeneity and isotropy. It aims at understanding, the origin, structure, composition, evolution, and fate of the Universe. Homogeneity means that the universe is the same place to place and isotropy means it looks the same in all directions. This assumption of the universe being homogenous and isotropic is important because observations made from any single point can be used to represent the universe as a whole and in turn this information can therefore be legitimately used in testing cosmological models. This theoretical assumption was made by Albert Einstein in his earliest work in the twentieth century and was meant to simplify the mathematical analysis (Amandola, 2021)

1.1.1 Geometry of our Universe

The geometry of the universe simply means its curvature which is denoted by k and its shape. The curvature can be positive, negative or zero. There are many shapes but only three basic ones are considered which are flat, open and closed shapes of the universe. In the year 1925, Edwin Hubble discovered that our universe is expanding. Hubble came up with evidence showing that the farther a galaxy is the faster it moves away from us and this is now known as Hubble law. The Hubble law simply means the rate of expansion of space and it applies to any system that expands and or contracts in a uniform and isotropic manner (Piattela, 2018). The equation (1) below describes the Hubble law.

$$v = H_0 r \tag{1}$$

where, v is the velocity it moves away from us, r the distance, and H_0 is the Hubble constant. The H_0 value as determined by recent measurements is, $H_0 = 67.6 \text{ Km/s/Mpc}$. This value means that for a Mpc away, a source moves away at a speed of 67.6 km/s faster.

Towards the end of 20th century, observations made on the radiation emitted from type Ia supernovae confirmed that the universe is expanding and discovered that this expansion is accelerating. This discovery about the accelerated expansion of the universe posed a great challenge in physics. There was need for cosmological models that could explain this anomalous because our knowledge on gravity is that it should attract matter, and that we should expect the expansion to decelerate (Shu W, 2015). One of the solutions settled on was

via the spacetime geometry structure in which length, time and mass are said to be related. It was assumed that there could be some form of new energy which is acting as anti-gravity called dark energy. Other observations from different sources and of different nature at different distances have indicated that there is dark component of matter called dark matter (DM). We can use this dark energy, and dark matter together with normal matter to obtain the universe's density parameter. The value of this parameter is derived by finding the ratio of the average total matter and energy density to the critical density. The critical density can be explained as density in which the universe would halt its expansion and that is only after an infinite time. See the equation (2) below.

$$\Omega_0 = \frac{\rho}{\rho_c} \quad (2)$$

Where, ρ and ρ_c are actual density and critical density of the universe respectively.

The value of this parameter density Ω_0 is almost one. There are studies going on aiming at finding on whether the value of Ω_0 is greater than 1, less than 1 or exactly 1, which in turn can give the geometry of the universe as follows;

1. $\Omega_0 < 1$ This means that the universe is open which tells us that it will continue to expand forever. An open universe's shape is likened to that of 3D saddle on which two parallel lines diverge.
2. $\Omega_0 > 1$ This means that the universe is closed which tells us that it will eventually stop its expansion and re-collapse. A closed universe's shape is likened to that of a 3D sphere in which two initially parallel lines will finally converge.
3. $\Omega_0 = 1$ This means that the universe is flat and that it has matter to stop the expansion but won't to re-collapse it. The shape of a flat universe is likened that of a flat sheet or Euclidean such that any two initially parallel lines on it will always remain parallel to each other.

$$\Omega_0 = \Omega_\rho + \Omega_k + \Omega_\Lambda \quad (3)$$

where, Ω_ρ is matter density, Ω_k dark energy density/ curvature density and Ω_Λ is cosmological density.

1.1.2 The Cosmic Microwave Background

The cosmic microwave background (CMB) is the electromagnetic radiation remained after the Big bang. This radiation is a powerful tool in investigating the early universe and the information obtained is used in constraining the standard cosmological model parameters. The CMB radiations gives us a picture on how the universe looked like when it was a few hundreds of thousands years of age, a time at which the neutral atoms could form and photons decouple from matter. This CMB radiation was found to have black body spectrum by Cosmic background explorer (COBE) satellite from which it can be concluded that matter and radiation balanced in the early periods. So the distribution of photons should reflect that of matter at the time decoupling took place and if there is an inhomogeneity in matter density it means that fluctuations of CMB temperature occurred.

In the early 1990s, COBE detected anisotropy in the CMB temperature, though the level was very small, it made it simple to predict theoretically anisotropy pattern by applying linear perturbation theory. This anisotropy pattern gives cosmological information which is mostly concentrated at angular scales which is less than a degree on the sky and this corresponds to the perturbations that were inside the horizon before decoupling. It is through these scales that physical processes left CMB imprint in the early Universe.

The CMB power spectrum shape is determined by the cosmological parameters. With perturbations in density, given its initial distribution in the early Universe, the relative peaks' height indicates baryonic matter density in the Universe. However, the peaks' position depends on the mapping of the sound horizon's physical scale into angular dimensions on the sky at decoupling which also depends on the geometry of the Universe. For instance, in an open Universe, at decoupling, the angle of physical scales is small compared to that of a flat Universe. Therefore, the peaks' position of CMB power spectrum is a good approximation of the total density of the universe.

Planck's Legacy 2018 used the Gravitational lensing to measure the density matter of the Universe. Gravitational lensing can be defined as the process by which radiations from distant astronomical objects is bent by the gravity of massive objects it encounters as it travels towards us. This bending makes the images of background astronomical objects appear slightly distorted and such observations is used to obtain useful cosmological information. The degree at which CMB light has been bent or 'gravitationary lensed' while travelling through the universe over the past 13.8 billion years is what the Planck Telescope uses to measure and be able to gauge the density of the universe. The amount of matter that

intervenes CMB photons as they travel towards the earth, gives the extent at which they are deflected so that their direction does not crisply reflects their starting in the early universe (Balbi A, 2004).

1.1.3 Standard cosmological model

The current Standard Cosmological Model is denoted by Λ CDM, where Lambda (Λ) is a cosmological constant associated with dark energy and CDM is an abbreviation for cold dark matter which is the sufficient massive dark matter particles of the Universe. This model assumes that the origin of the Universe is from pure energy that underwent the Big Bang and that about 5% of it makes normal matter while 27% makes dark matter and 68% dark energy. This model assumes further that in the large scales the universe is not only homogeneous but also isotropic. This model is based on two theoretical models which are; the Standard Model of Particle Physics (SMPP) also called physics of the very small and General Theory of Relativity (GTR) which is the physics of the very large. However, these two models have their shortcomings. For instance, the SMPP does not give an understanding on how the three generations of leptons and quarks came to exist and even their mass hierarchy, nature of gravity and the nature of dark matter. GTR on the other hand is short of information about Big Bang cosmology, inflation, the asymmetrical of the matter-antimatter in the universe, and the nature of dark energy (Robson B, 2019).

1.2 Theory: History of cosmology

Looking into observational Cosmology, the first model to describe the universe was the 'island universe' model that was developed by Descartes that was published in *The World of 1636* which involved the solar system problem. In the year 1750 Wright published a book with a title *An Original Theory of the Universe* which involved stars and the solar system in a sphere. In 1755 Kant and 1761 Lambert came up with first pictures of the Universe which were hierarchical. All these information about the Universe did not have observational validation. Afterwards, the distance of the Sun was known, making it a first star with a known distance. Friedrich Bessel *et al.* (1830s) made the first parallax measurement of stars.

The quantitative estimations about scale and structure of Universe were made by William Herschel in 18th century. His large-scale structure model was based on the counting of stars and it gave an evidence for the 'island universe'. Herschel derived the famous model for the galaxy on an assumption that the absolute luminosities of the stars were the same.

John Michell, a Geology Woodwardian Professor at Queen's College, Cambridge, warned William Herschel on his assumption that stars had fixed luminosity. In 1767, John Michell developed the Cavendish experiment which was used to measure the average Earth density. Michell is greatly remembered from his invention of black hole. In 1802, Herschel after measuring the visual binary magnitudes of our Galaxy and stars, in his conclusion he agreed with John Michell's warning about the luminosity of stars and finally he lost faith in his model.

Throughout the 19th century there was a great desire to make observations of the Universe using a telescope of a higher aperture. A 72-inch reflector, the largest telescope then was constructed by William Parsons at Birr Castle, Ireland. The telescope was so big that on tracking the astronomical objects, its barrel was moved by ropes so as to accommodate the platform that could move at the Newtonian focus of the telescope during observations. During this century, the problem of pointing of reflecting telescope was solved by Lewis Morris Rutherfurd, Andrew Common, John Draper and George Carver by inventing plate holder which was adjustable that enabled the observer to maintain pointing and high precision.

The advancement in technology is attributed to achievement made by James Keeler; he was able to obtain spiral nebulae images among them was his famous M51 image. The images showed detailed structures of the spiral nebulae in which a large number were fainter at a smaller angular size. He concluded that, if these fainter objects were similar to Nebula M31 of Andromeda, then they farther away from the solar system.

Carnegie discovered helium through astronomy long before it was identified in the laboratory. This is one way to prove that astronomy can provide information about behavior of matter by just making astronomical observations which can be reproduced later in the laboratory. Carnegie facilitated the construction of 100-inch Hooker Telescope, which was the largest in the world with all other features learned from other earlier telescopes. In the year 1918, it was complete and it dominated for about 30 years until 1948 another larger telescope, Palomar 200-inch telescope was commissioned.

Using 100-inch Hooker Telescope, Scheiner (1899) obtained M31 spectrogram and stated that it suggested Sun-like stars cluster. Opik, in 1922 compared mass-to-light ratio of M31 with our Galaxy and obtained an estimate distance of M31 to be 440 kpc. The same year, Duncan discovered variable stars in spiral nebulae that in turn led to a discovery by Hubble of variable stars in M31.

A paper by Hubble (1925&1926) provided a description about galaxies in the extragalactic system. The paper classified the galaxies into Hubble types with an estimation number of the different types, their mass-to-luminosity ratio and average densities. Its at this time the mean mass density of the Universe as a whole was derived. By the year 1929, after Hubble collecting approximation distances of about 24 Galaxies with measured velocities he came up with his law that bears his name; the Hubble law.

Theoretical cosmology is attributed to Albert Einstein with his famous static model of the Universe. First, in the year 1825, Lobachevsky and Bolyai violated the Euclid's fifth axiom by solving the problem of existence of geometries. Their work led to an introduction of quadratic differential forms by Riemann resulting to the generalized non-Euclidean geometries. After a long rout of searching for a consistent theory of gravity that was relativistic using ideas such as; the influence of gravity on light, the principle of equivalence, and the Riemannian spacetime, Einstein came up with general relativity. As the year 1912 was ending, he wanted to have a non-Euclidean geometry. He consulted his friend Marcel Grossmann, on a general way to transform frames of reference for metrics of the form

The Grossmann's answer was that Einstein should use the Riemannian geometries, though they were nonlinear a fact Einstein took as an advantage because any theory that satisfies relativistic gravity must be nonlinear. In the year 1915 Einstein formulated general relativity in its definitive form. In the following year, Willem de Sitter and Paul Ehrenfest gave an idea that in order to remove the problems of the boundary conditions at infinity, there has to be a spherical 4-dimensional spacetime. In 1917, Einstein realized that general relativity was a theory that can be used to construct consistent model of the Universe. At this time the expansion of the Universe was yet to be discovered.

$$ds^2 = g_{\mu\nu} dx^\mu dx^\nu \quad (4)$$

In his theory, Einstein wanted to incorporate the fact that, in the large-scale Universe, distribution of matter should determinate the local inertial frame of reference. Another problem emerged; Newton noted that a static model of the Universe is unstable under gravity. This forced Einstein to introduce another term called the cosmological constant denoted by Λ into the field equation that solved the problem.

$$\frac{d^2R}{dt^2} = -\frac{4\pi G\rho_0}{3R^2} + \frac{1}{3}\Lambda R \quad (5)$$

In the same year, de Sitter found the solutions of Einstein's field equations in the absence of matter $\rho = p = 0$ meaning that Einstein did not achieve his objectives. de Sitter's metric was in the form

$$ds^2 = dr^2 - R^2 \sin\left(\frac{r}{R}\right)(d\phi^2 + \cos^2 \phi d\theta^2) + \cos^2\left(\frac{r}{R}\right)c^2 dt^2 \quad (6)$$

In 1922, Kornel Lanczos interpreted de Sitter solution by coordinate transformation as follows.

$$ds^2 = -dt^2 + \cosh^2 t [d\phi^2 + \cosh^2 \phi (d\psi^2 + \cos^2 \psi d\chi^2)] \quad (7)$$

In the same year, Alexander Alexandrovich Friedmann wrote a paper about relativistic cosmology. He noted that for an isotropy world model, the curvature has to be isotropic. He formulated model showing a solution of expanding world with closed spatial geometrie.

$$\frac{3\dot{R}^2}{R^2} + \frac{3c^2}{R^2} - \Lambda = kc^2\rho \quad (8)$$

On solving these equations one can get exactly the standard world models of general relativity. In 1927, Georges Lemaître also discovered the solutions of Friedman. Lemaître and Howard P. Robertson in 1928 became aware that the Friedman solutions were actually a discovery that was taken as an evidence for the expansion of the universe. In 1935, Robertson and George Walker independently solved the problem of time and distance in cosmology. For homogeneity and isotropy world, they introduced a metric of the form

$$ds^2 = dt^2 - \frac{R^2(t)}{c^2} \left[\frac{dr^2}{1 + k r^2} + r^2 d\theta^2 + r^2 \sin^2 \theta d\phi^2 \right] \quad (9)$$

where k is the space curvature at the present epoch, r is a radial distance of comoving coordinate and R(t) is proportional to the distance between any two worldlines changing with cosmic time t and is scale factor, (Longair S, 2004).

Cosmology uses the Friedmann-Lemaitre-Robertson-Walker (FLRW) cosmological model in understanding the evolution of the universe. This model is so successful and for that reason it has become the standard cosmological model which now is used to predict about the universe even at earliest times of 10^{-43} sec after the Big Bang (Piattela, 2018).

It is until towards the end of the twentieth century when firm empirical data was obtained to confirm the homogeneity and isotropy of the universe exactly the same as the Cosmological Principle had predicted. The temperature of the cosmic microwave background (CMB) radiations which is uniform serves as the best evidence for the isotropy of the observed universe.

1.3 Statement of the Problem

The standard cosmological model Λ CDM predicts the shape of the universe to be flat which agrees with many cosmological observations. The knowledge of the shape of the universe is of great importance as it can be used to predict the evolution and fate of the universe which is in continuous accelerated expansion and it depends on the density parameter. However, the recent cosmological observations, from The Planck Legacy 2018 data indicates that, the Cosmic Microwave Background light's amplitude is larger. This can only be explained by the closed universe model. This poses a challenge to the current Standard cosmological Model. Therefore, there is a lot of concern to both observational and theoretical cosmologists that the present model which assumes the shape of the universe to be flat may be incomplete or inaccurate. This concern has shifted our focus to thorough scrutiny through research on whether the current model is incorrect and if so then what will be its implications in cosmology. Although the recent data has suggested possible model of a closed universe, more observations are required to ascertain these claims. In this research we aim to explore the evidence of a closed universe and see if there could be crisis in cosmology.

1.4 Objectives

1.4.1 Main Objective

The main objective of this work is to explore the evidence of the closed universe as suggested by Planck Legacy 2018 data, which shows enhanced amplitude of CMB, and establish a model of a closed universe.

1.4.2 Specific Objectives

Specific objectives of this study are:

- 1 To derive equations governing dynamics of a closed universe within Einstein Theory of General Relativity considering isotropy and homogeneity.
- 2 To obtain equations governing the evolution of matter density and matter density contrast of the universe.
- 3 To derive the equations and develop relevant theory behind possible crisis with regard to the proposed evidence of a closed universe.
- 4 To study the implications of the closed universe evidence for current cosmology.

1.5 Justification and Significance of the Study

The shape of the universe is key on formation of a standard cosmological model which gives the insight of the dynamics and the future of the universe. The universe is flat an assumption made by the current Standard Cosmological Model Λ CDM. Considering the importance of the model of the shape of the universe in cosmology, the valid way to explain the abnormality in PL18 is to model a closed universe shape. Exploring PL18 is of great significance because: It will help challenge the existing model of a flat universe and shift to a closed universe model; It will help us to predict the future and fate of the universe as the accelerated expansion of the closed universe will halt and Big Crunch occur; It will help to solve the problem of the enhanced amplitude in CMB by PL18.

CHAPTER TWO: LITERATURE REVIEW

The General Theory of Relativity by Albert Einstein, explains how mass can curve the space (Peacock, 1999). If we can find out by how much mass is spread over the entire volume, then the universe's matter density can be found out. Therefore, the measure of the universe's expansion and density is used to determine its shape as well as its fate.

In 2013, The Planck Collaboration issued a report on the CMB radiation in which, according to the report, their maps had the highest precision due to the increased resolution. This report was based on the standard cosmological model, Λ CDM framework in which the data from Planck indicated that Hubble constant H_0 was not in agreement with many other measurements that were done directly to probe H_0 . They concluded that for such problem to be resolved the dark energy model together with its equation of state (EoS) denoted by w should not be equal to -1 was a requirement. According to the report, if it is assuming that w is a constant, then this data would favor $w < -1$ at 2 standard deviation confidence level if it was to be combined with the supernovae "SNLS" compilation. Therefore, the value of H_0 $H_0 = 71.3 \pm 2.0 \text{ km s}^{-1} \text{ Mpc}^{-1}$ (68% C.L.) agreed to that from direct probes.

In the article by (Jun-Qing, 2013), w was obtained with 68% C.L. constraints $w_0 = -0.81 \pm 0.19$ and $w_\alpha = -1.9 \pm 1.1$ which was from both the Planck's data and the "SNLS" compilation.

In the Planck collaboration of 2013 was the first cosmological papers that provided not only the highest resolution but also the data was from the full sky and the maps from CMB temperature anisotropies. In this way, the Planck data was able to constrain many of the cosmological parameters at little percent level and as a result were able to improve the value of H_0 , namely $H_0 = 67.4 \pm 1.4 \text{ km s}^{-1} \text{ Mpc}^{-1}$ at 68% C.L. But still this result was not in agreement with those measured by other lower-redshift methods, an example the the probe that was done on H_0 by Hubble Space Telescope (HST) which had $H_0 = 73.8 \pm 2.4 \text{ km s}^{-1} \text{ Mpc}^{-1}$ or $H_0 = 74.3 \pm 1.5(\text{stat.}) \pm 2.1(\text{sys.}) \text{ km s}^{-1} \text{ Mpc}^{-1}$. They concluded that this difference might be due to unknown systematics in measurements and if not, then the discordance between measurements of H_0 could imply that the flat Λ CDM model could be incomplete. Therefore, for a constant EoS that represented dark energy model, H_0 in the CMB depends on a model hence the value of H_0 keeps on changing.

In a paper by (Ade P.A.R, 2016), also presented Planck observations and cosmological results which were based on anisotropies of temperature and polarization in the cosmic microwave background (CMB) radiation.

These results agreed with the analysis that was conducted in 2013 on data which was from the Planck nominal-mission temperature. They found out that, increase in accuracy, both temperature and power spectra polarization agreed with the standard Λ CDM model denoted “base Λ CDM”. On combining temperature data from Planck with that of Planck lensing, they found a Hubble constant, $H_0 = (67.8 \pm 0.9) \text{ kms}^{-1}\text{Mpc}^{-1}$, and the value of the matter density parameter $\Omega_m = 0.308 \pm 0.012$, with spectral index $ns = 0.968 \pm 0.006$, which was consistent with the 2013 analysis.

In the report, they indicated that the neutrino masses’ sum was restricted to $\Sigma m_\nu < 0.23 \text{ eV}$. And that the curvature of the universe approached zero, with $|\Omega_k| < 0.005$. They added a tensor component that was extended to base Λ CDM and they got an upper limit on the tensor-to-scalar ratio to be $r_{0.002} < 0.11$, which was in agreement with the results from Planck 2013 and polarized B-mode data which had been analyzed jointly by BICEP2, Keck Array, and Planck (BKP). After they added the data from BKP B-mode to their analysis they were able to reduce the constraint to $r_{0.002} < 0.09$ in which the inflationary model was not favored. The combination of astrophysical data and that from Planck, they found the EoS of dark energy to be restricted to $w = -1.006 \pm 0.045$, a value that was in agreement the average for a cosmological constant.

It was found that results from Planck for base Λ CDM agreed with BAO data and the JLA sample of Type Ia supernovae. Even though, fluctuation spectrum amplitude was larger than that inferred from other analyses e.g. gravitational lensing. They resolved that such a tension cannot just be removed by simple modification of the base Λ CDM cosmology.

They drew conclusions as follows

- The base Λ CDM model was good approximation that matches the 2015 Planck data.
- By comparing the TE and EE spectra which were computed by finding a difference in frequency combinations, they found out that the systematic effects were due a leakage of temperature-to-polarization and hence the Planck 2015 TT, TE, EE, and lensing spectra agreed with each other based on the base Λ CDM cosmology.

- The reionization optical depth given by $\tau = 0.066 \pm 0.016$ and a reionization redshift given by $z_{re} = 8.8_{-1.4}^{+8.8}$ agreed with those from WMAP9 polarization data which also in agreed with the Planck temperature and lensing data results.
- The Planck 2015 HFI spectra were found to be higher by 2 % in comparison to 2013 data.
- TT, TE, and EE from Planck was an accurate description of an adiabatic spectrum of fluctuations giving tilt index to be $n_s = 0.968 \pm 0.006$, which agreed with the predictions made from the single-field inflationary models.
- The base Λ CDM cosmology was in good agreement with results from BAO surveys and JLA sample of Type Ia SNe.
- By combining the data from Planck TT+lowP+lensing with other astrophysical data, EoS for dark energy was restricted to value of $w = -1.006 \pm 0.045$ that is compatible with a cosmological constant based on the base Λ CDM cosmology.

Another paper by (Che-Qiu 1, 2019), about the Hubble Parameter H_0 tension in the infinite future suggested an existence of a constant value of $H(z)$ at $z = -1$ when in ω CDM universe with $\omega > -1$, which did not dependent on other cosmological parameters. They performed what is known as the model-independent Gaussian Processes (GP) by combining the theoretical $H(z)$ value with other 43 observational $H(z)$ data (OHD) values that were latest by then and they constrained the Hubble constant in and obtain $H_0 = 67.6 \pm 3.03 \text{ km s}^{-1} \text{ Mpc}^{-1}$, a value which agreed with H_0 values from Planck Collaboration (2015). Using Markov Chain Monte Carlo (MCMC) method, they performed χ^2 statistics on H_0 value in which they obtained $\Omega_m = 0.26 \pm 0.02$ and $\omega = -0.85 \pm 0.06$ based on flat ω CDM model, and $\Omega_m = 0.27 \pm 0.04$, $\Omega_\Lambda = 0.80 \pm 0.12$ and $\omega = -0.82 \pm 0.07$ based on a non-flat ω CDM model, and found that this values were larger compared to those that did not use the theoretical $H(z)$ value.

They concluded that, H_0 value was in agreement with both Planck Collaboration (2015) result and the one year older then latest Planck Collaboration (2018) result ($H_0 = 67.4 \pm 0.5 \text{ km s}^{-1} \text{ Mpc}^{-1}$). However, in this exploration, still the Hubble constant tension remained unsolved. They suggested that more observations and improved data processing methods were required which could lead to a more precise Hubble constant values.

Another key paper in this work is the report by (Di Valentino E, 2019) that explored the evidence for a closed Universe and tried to understand whether there could be a possible crisis for cosmology in which the data was obtained by the Planck legacy 2018. According to this paper, the data from Planck observation's telescope in the recent Planck Legacy 2018 confirmed enhanced lensing amplitude to be present in the CMB power spectra as opposed to that predicted in the standard Λ CDM model. The only way this effect could be explained physically is through a closed universe in which now Planck CMB spectra preferred a positive curvature at more than 99% C.L.

The aim of this paper was to investigate this evidence for a closed universe and be able to show whether the positive curvature could explain the anomalous lensing amplitude. Di Valentino *et al.*(2019) wanted to show whether the discordances in Planck data which preferred a closed universe, had risen from local observations in cosmology due to the assumption of a flat universe and whether could there was a cosmological crisis which could need future measurements to clarify these discordances or they were simply due to undetected systematics, or to new physics, or simply are a statistical fluctuation.

This paper claimed that the preference for higher lensing amplitude as data from Planck Legacy 2018 suggested could lead to new physics beyond the so-called Λ CDM standard cosmological model. This “ A_{lens} ” anomaly could imply that the Λ CDM model could require an extension because all constraints from that of PL18 CMB spectra on curvature, to the energy density parameter Ω_K , had 3.4 standard deviations ($-0.007 > \Omega_K > -0.095$ at 99% C.L.) pointing towards a closed universe.

The problem with the closed models is that the primordial density fluctuations require a large-scale cut-off. $R_c = (\frac{c}{H_0})|\Omega_K| - 0.5 \sim 10$ Gpc. And that the current cosmological parameters constraints are obtained by combining data sets which needs to be consistent. As of now according to this paper the main data sets that did not agree with Planck are two namely; Hubble constant at about 3 standard deviations and cosmic shear by the KiDS-450 survey with 2 standard deviations.

According to this paper, cosmological crisis could be masked by the fact that the suggestion of PL18 CMB spectra curvature will allow the statistical significance to vary and thus increasing the known tensions with PL18 and this would be inconsistent with the assumption of a universe being flat. For a flat model with $\Omega_m = 0.35, \Omega_\Lambda = 0.65$ and $H_0 = 65$ km/s/Mpc would produce a similar structure of the CMB angular spectrum for a closed model with

$\Omega_m = 1$, $\Omega_\Lambda = 0.15$ (i.e. $\Omega_k = -0.15$) and $H_0 = 38.4$ km/s/Mpc if the inflationary parameters and reionization process was to be assumed and this could make the posterior of the parameter Ω_k skewed towards closed models after marginalization.

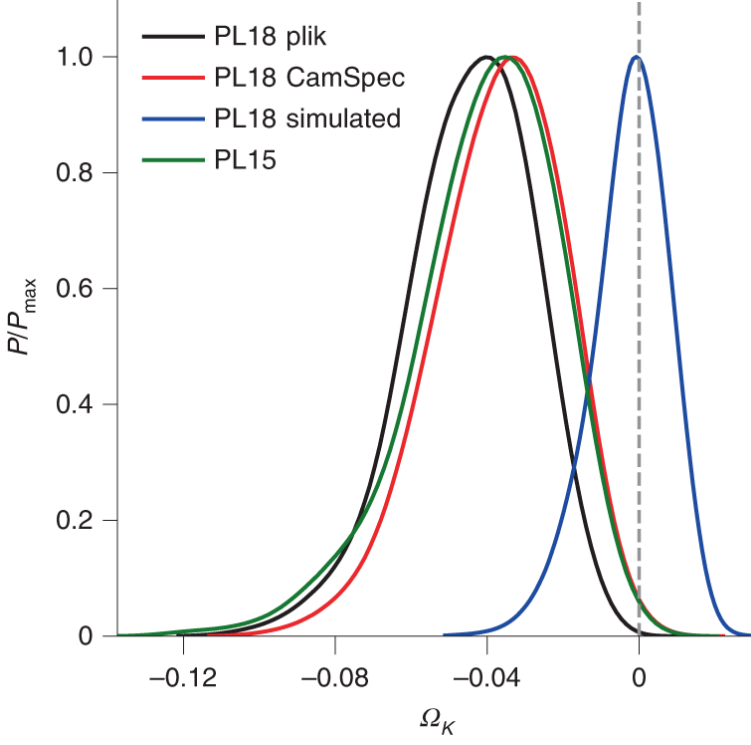


Figure 2. 1: Preference for a closed universe (Di Valentino E, 2019).

Di Valentino *et al.*(2019) pointed out that induced anisotropies that could not be neglected because this bending of CMB light depends on the density of the matter and the degeneracy in geometry could be broken by its detection. The plot above in **figure 2.1**, the posterior was from the temperature of PL18 and polarized power spectra which was preferred a closed model at about $\Omega_k = -0.04$, and this is when they assumed the Planck likelihood baseline. After integrating this posterior they found out that the distribution over Ω_k , from Planck favored a closed Universe ($\Omega_k < 0$) with a probability of 99.985%. This positive curvature universe with parameter $\Omega_k = -0.0438$ provided a better fit as far as PL18 was concerned with respect to a non-curved model, and it had a χ^2 difference of $\Delta\chi^2_{\text{eff}} \sim -11$.

To account for the Bayesian complexity they used the Deviance Information Criterion (DIC) in order to quantify the preference for positively curved model as shown below.

$$DIC = \text{ave}(2 \chi_{\text{eff}}^2) - \chi_{\text{eff}}^2 \quad (10)$$

where χ^2_{eff} is the chi-square best-fit from the MCMC chains which is a mean over the posterior distribution. This analysis was restricted to curved models within the range $-0.2 \leq \Omega_k \leq 0$. The results from Planck data yielded $\Delta DIC = -7.4$, which means that for a positively curved universe with $\Omega_k = -0.0438$ was preferred with about 1:41 a ratio with respect to a flat model.

They also computed the Bayesian Evidence ratio using the Savage-Dickey density ratio (SDDR) as shown.

$$B_{01} = \frac{|p(\Omega_k | d, M1)|}{\pi(\Omega_k | M1)|\Omega_k} = 0 \quad (11)$$

Here, M_1 is the model with curvature, while $p(\Omega_k | d, M1)$ is the posterior for Ω_k , and $\pi(\Omega_k | M1)$ is the prior on Ω_k that they assumed as flat within the range $-0.2 \leq \Omega_k \leq 0$. And the Planck temperature and polarization Bayes ratio from Savage-Dickey method was:

$$| \ln B_{01} | = 3.3 \quad (12)$$

In this paper, another approach called CAMSPEC was used instead baseline one by Planck likelihood, although the preferred curvature reduced but still was more than 2 standard deviations with $\Omega_k = -0.037^{+0.032}_{-0.034}$ at 95% C.L. To show that the result was not due to different methods of analysis, with CAMSPEC they obtained, $\Omega_k < 0$ with a 99.85% probability and this indicated that the universe is closed.

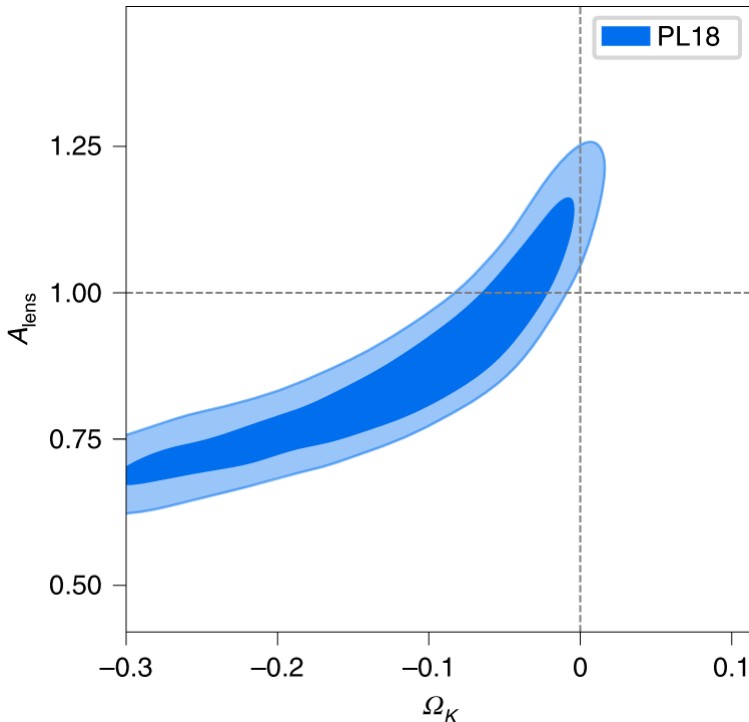


Figure 2. 2: Degeneracy between curvature and lensing (Di Valentino E, 2019).

The **figure 2.2** above as per Di Valentino *et al*, (2019) report showed a discordance between curvature and the A_{lens} to be present at 68% and 95% constraints in the A_{lens} vs Ω_k plane from temperature of Planck 2018 and polarization data in which the model with $\Omega_k < 0$.

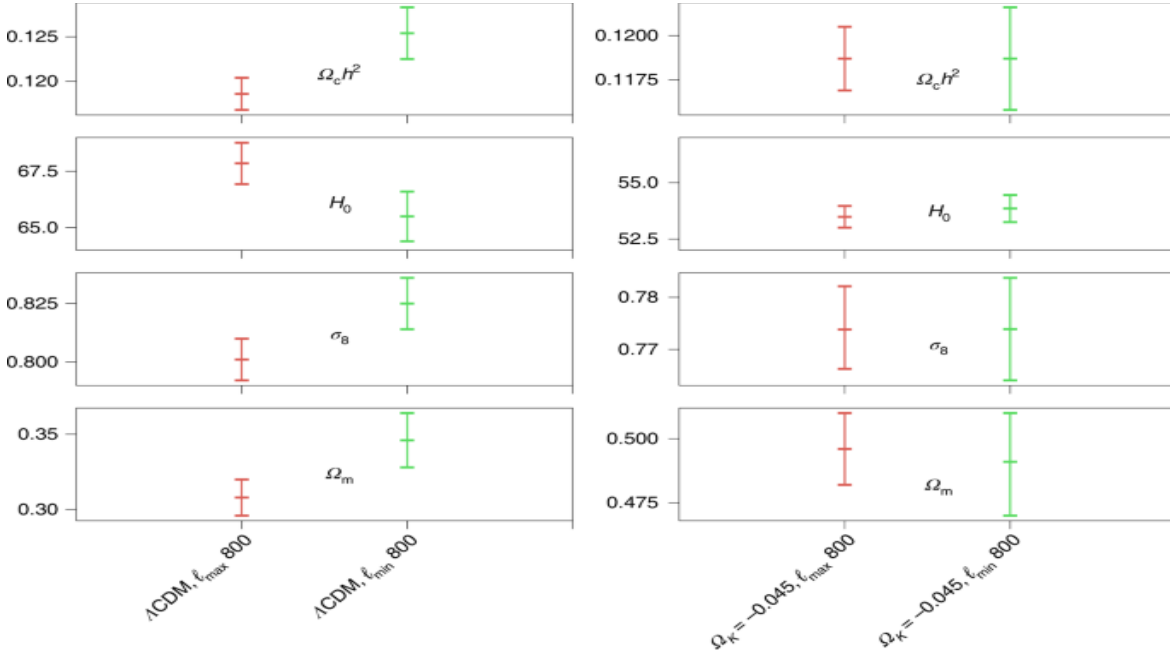


Figure 2. 3: Curvature and parameters shift (Di Valentino E, 2019).

Figure 2.3 shows the relationship between two cosmological parameters that ranges ($2 \leq l \leq 800$ and $800 < l \leq 2500$) of the data of polarization and temperature from Planck 2018 that assume a Λ CDM model on the left and a closed model on the right. However, in this report they noted that that a Λ CDM+ Ω_K provided a marginally better fit compared to to the Λ CDM+ A_{lens} by analysis $\Delta\chi^2 = -1.6$.

They noted that r was a drag of the comoving sound horizon at the time of the end of the baryon drag epoch and D_V combined the Hubble parameter $H(z)$ and the comoving angular diameter $D_M(z)$, this was after they had plotted the ratio $D_V(z)/r_{\text{drag}}$ as a function of redshift z , that which had extracted from a recent BAO surveys, and afterwards divided a mean a ratio

which they obtained by Planck temperature and polarization data using a Λ CDM+ Ω_K model as shown in equation (6)

$$D_V(z) = \frac{(czD2M(z))}{(H(z))^{1/3}} \quad (13)$$

PL18 power spectra did not agree BAO data when the curvature was assumed and the PL18 χ^2_{eff} best-fit was worse with a huge value of $\Delta\chi^2 \sim 16.9$ and from this they said that they could not obtain directly the number of independent data points that was found in the BAO dataset and at the same time be able to approximate the tension between the data sets from a simple χ^2 analysis. They checked the consistency between two independent data sets D_1 and D_2 by evaluating the quantity below based on the DIC approach.

$$F(D_1, D_2) = DIC(D_1 \cup D_2) - DIC(D_1) - DIC(D_2), \quad (14)$$

In the above equation $DIC(D_1 \cup D_2)$ was the DIC obtained by analysis of combination of the data sets.

With the Jeffrey's scale, it follows, if $|\log_{10}I| > 0.5$, strong if $|\log_{10}I| > 1.0$ and 'decisive' if $|\log_{10}I| > 2.0$ and the explanation for this was that, if $\log_{10}I$ was positive then the two data sets agreed and if not then were in tension. The results were that models without curvature agreed by ($\log_{10}I = 0.2$) while those with curvature disagreed with $\log_{10}I = -1.8$ between BAO data and that from Planck

Here, Λ CDM model also agreed with CMB lensing, but again for the PL18 best fit $\Omega_k = -0.0438$ model predicted a large amplitude. After including the CMB lensing to PL18 the best fit chi-square increased by $\Delta\chi^2 = 16.9$ and this suggested the presence of tension at the 95% C.L. in the case of Λ CDM+ Ω_K . In their observations they identified that there was an agreement between PL18 and CMB lensing for a flat Universe case where ($\log_{10}I = 0.6$) and this changed to discordance ($\log_{10}I = -0.55$) when they allowed a curvature to vary. See the table below.

Additional database	$\Delta\chi^2_{\text{eff}}$	ΔN_{data}	$\log_{10} I$
flat Λ CDM			
+BAO	+6.15	8 0	0.2
+ CMB Lensing	+8.9	9	0.6

Λ CDM+ Ω_K			
+BAO	+16.9	8	-1.8
+ CMB Lensing	+16.9	9	-0.84

Table 2. 1: Tensions between PL18 and BAO and CMB Lensing.

The **figure 2.4** below was used by Di Valentino *et al*, (2019) to show that the model Λ CDM+ Ω_K provided the constraint: $H_0 = 54.4^{+3.3}_{-4.0}$ at 68% C.L in PL18 power spectra which was in disagreed at about 5.2 standard deviations and $H_0 = 73.52 \pm 1.62$ at 68% C.L.

The same scenario was observed with a shear in cosmic data from KiDS-450 where an increase in the tension was observed.

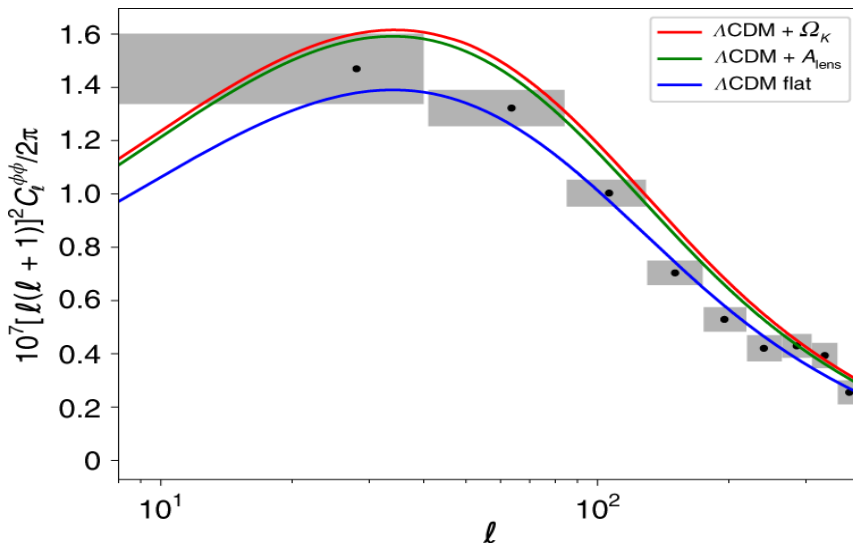


Figure 2. 4: Tension with CMB lensing (Di Valentino E, 2019).

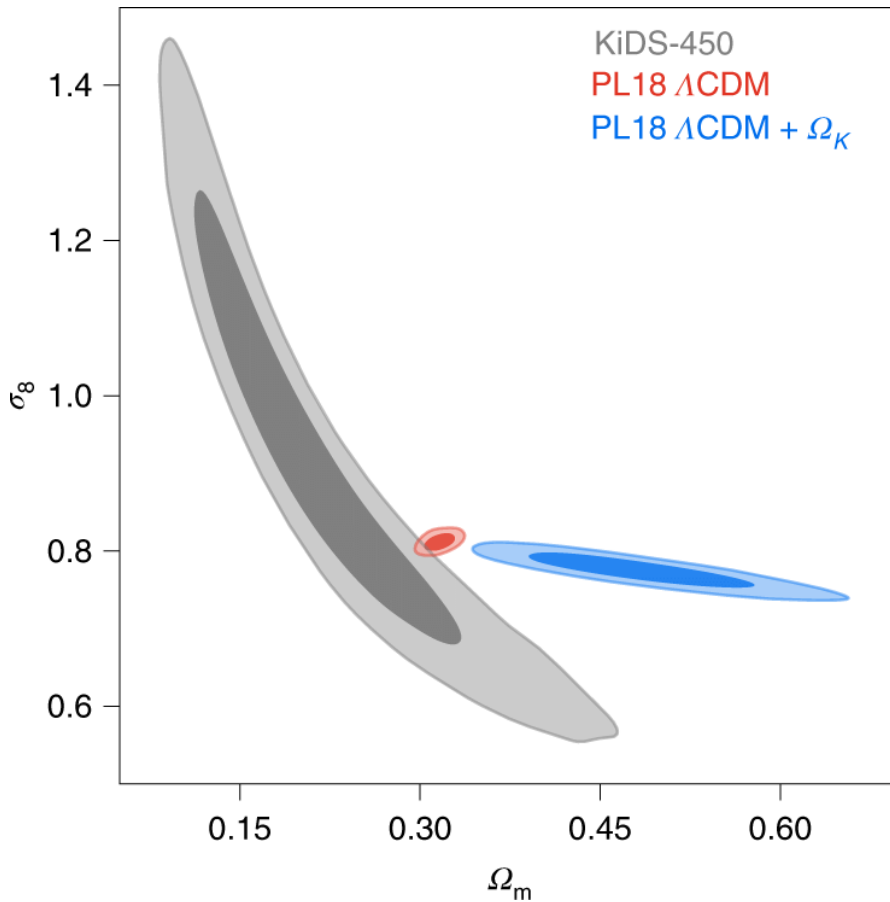


Figure 2. 5: Tension with cosmic shear measurements (Di Valentino E, 2019)

Di Valentino (2019) obtained $S_8 = 0.981 \pm 0.049$ at 68% C.L. from power spectra of the PL18 and from the KiDS-450 result the value was found to have a 3.8 standard deviations. However, the Cosmic shear measurements that was done by the Dark Energy Survey (DES) and another by the Subaru Hyper Suprime-Cam (HSC) was in agreement with the PL18 result but only with a flat Universe. They arrested this problem by combining multiple datasets with Planck data and they obtained a confidence region at region at 95% C.L.as shown in the **figure 2.6** below and this was from a BAO+SN-Ia+BBN dataset where about 68% and 95% C.L. as per the PL18 power spectra on the Ω_K vs H_0 plane.

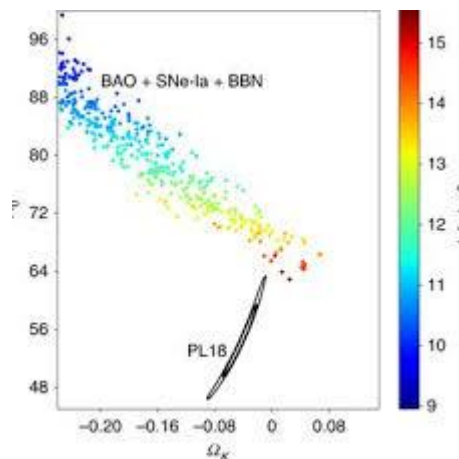


Figure 2. 6: Tension with combined data (Di Valentino E, 2019).

In this analysis Planck result did not agree with BAO+SN-Ia+BBN , and each data set preferred a curved Universe, with BAO+SN-Ia+BBN data set providing only an upper limit of $\Omega_k < -0.124$ at 68% C.L. It was concluded that the Planck result is preferred a Hubble constant value of $H_0 = 54^{+3.3}_{-4.0}$ km/s/Mpc at 68% C.L. and that the combination preferred lower ages of the universe.

They said that in **Figure 2.6** probability contour plots were broad from the BAO+SN-Ia+BBN analysis and that the CMB lensing and the R18 determination of the Hubble constant were considered, separately as shown in **figure 2.7**.

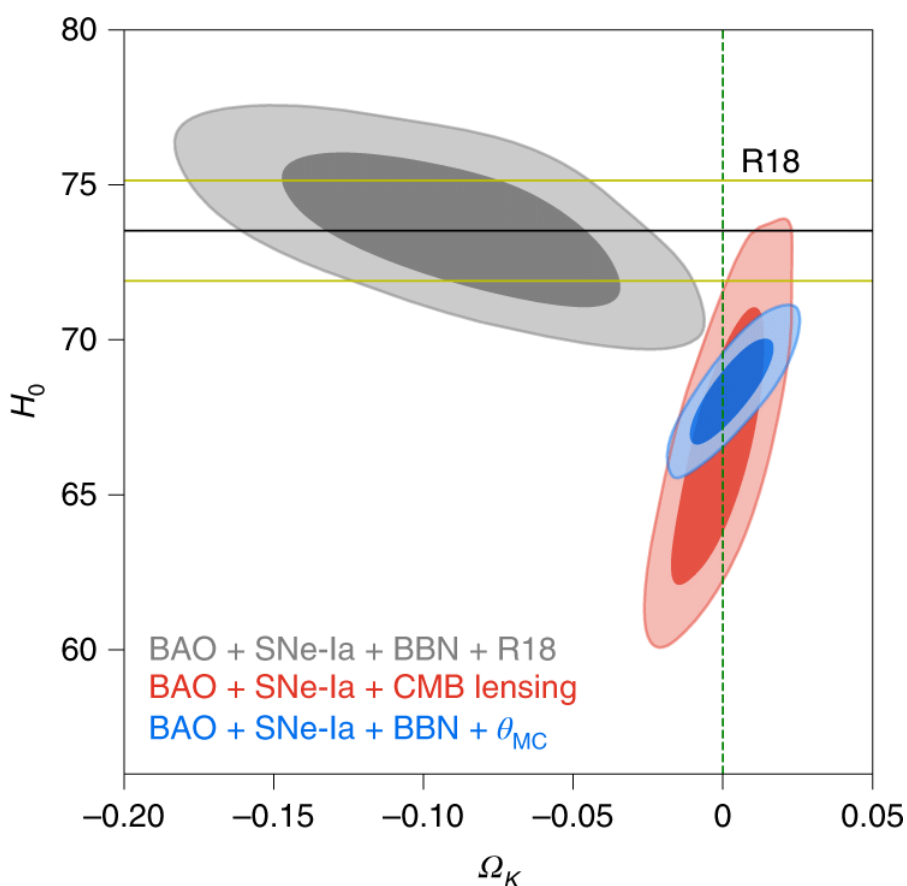


Figure 2. 7: Tensions in combined data (Di Valentino E, 2019).

In summary,

1. They found out that the PL18 CMB power spectra indicated the possibility of a closed universe.
2. They concluded that a closed universe could solve the disagreement in the Planck data.

3. They also argued that there was no local cosmological observables that favored them.
4. They resolved that a closed universe possibility could be due to discordance with PL18
5. They agreed that the inconsistencies was problem that could lead to an introduction for modern cosmology in which future observations can solve

From this paper by Di Valentino et al, (2019) we note that the large amplitude in relation to that of flat Λ CDM challenges the Friedmann Lemaître-Robertson-Walker (FLRW) model (Kolb E. W, 1989).

Another recent paper by (Heinesen & Buchert , 2020) also noted a tension between the Hubble parameter between observations made locally and those made by Planck which had 5 standard deviation (5σ) and according to them, this inconsistencies may be as a result of systematic effects whose origin is astrophysical and they might be influencing the Planck CMB power spectra at small angular scales which may lead to failure of FLRW model.

In this paper, they aimed at exploring the FLRW model curvature by showing how, what they called ansatz, violated the generic relativistic spacetime. Also they intended to explain how to modify volume-averaged spatial curvature using the FLRW conservation equation through structure formation for volume-averaged spatial and be able to illustrate how to solve the tension in FLRW spacetime using General Relativity and this could be achieved only if spatial curvature parameter Ω_{k0} in early-time was that preferred in Planck power spectra.

In their paper they highlighted a fact that curvature in FLRW cosmology has to be differentiated to that in generic relativistic spacetimes and they focused mostly on spacetimes with a single source of irrotational dust.

In general relativity according to their argument, the Riemann tensor tells us about the curvature of spacetime, while in cosmology the six vector fields which represent translational and rotational invariance in FLRW metric is assumed to reduce space metric solution and the spatial hypersurfaces of the Riemann tensor is calculated by finding the three-dimensional Ricci scalar $R = \frac{6k}{a^2(t)}$ and k is constant-curvature parameter., while $a(t)$ is scale factor that depends on time t .

The value k gives different topologies i.e. $k > 0$ means a hypersphere topology, $k = 0$ means flat, and $k < 0$ means a space which is hyperbolic. They argued that the FLRW 3-dimensional Ricci scalar is conserved $Ra(t)^2 = const$. The equation below is an irrotational dust spacetime of single source with four-velocity u .

$$\frac{1}{a_D^6} (Q_D a_D^6) \cdot + \frac{1}{a_D^6} (\langle R \rangle_D a_D^2) \cdot = 0 \quad (15)$$

And here R denotes a 3-dimensional Ricci scalar for hypersurfaces space which is perpendicular to the four-velocity fluid, and the operation $\langle R \rangle_D$ is Riemannian average, while D is domain of hypersurfaces space, and the $\cdot \equiv d/d\tau$ denotes the derivative with respect to the proper time. The scale factor on the domain can be found by its volume which is normalized by the initial volume as shown:

$$\frac{|D|}{|D_i|} =: a_D^3. \quad (16)$$

Q_D is the rate of expansion variance and the averaged fluid congruence shear scalar over the domain D ,

$$Q_D \equiv \frac{2}{3} \langle (\theta - \langle \theta \rangle_D)^2 \rangle - 2 \langle \sigma^2 t \rangle_D \quad (17)$$

And $Q_D = 0$ for expanding fluid which is isotropic, and structureless which reduces to the conservation equation of FLRW.

$$(\langle R \rangle_D a_D^2) \cdot = 0 \quad (18)$$

In this paper, it was pointed out that in dark energy and dark matter directions, the FLRW models are gravitationally unstable and it was noted that $\langle R \rangle_D$ can change sign over cosmic epoch due to relativistic spacetimes having generic feature something that is not possible in the FLRW class of models.

In their scheme they replaced the local spacetime variables of inhomogeneous cosmology by representing the ‘macro-state’ with volume-averaged variables. They said that local spacetime variables constrain global dynamics which obey the Einstein equations.

$$G_{\mu\nu} + \Lambda g_{\mu\nu} = 8\pi G T_{\mu\nu} \quad (19)$$

CHAPTER THREE: THEORETICAL FRAMEWORK

3.1 Einstein Field Equations

the Einstein Field Equations (EFE) which gives a relationship between Einstein tensor and Einstein tensor that describes the energy, all together gives the dynamics and evolution of the background universe, (Scott, 2003).

$$G_{\mu\nu} + \Lambda g_{\mu\nu} = 8\pi G T_{\mu\nu} \quad (20)$$

Where, $G_{\mu\nu}$ and $R_{\mu\nu}$ are the Einstein and the Ricci tensors respectively. Ricci tensor is metric and depends on its derivatives, R is scalar found by contracting the Ricci tensor

$$R = g^{\mu\nu} R_{\mu\nu},$$

G is Newton's constant; and

$T_{\mu\nu}$ is tensor called energy-momentum.

The equation (20) above describes fully what the universe is composed of.

3.2 Friedman–Lemaitre–Robertson–Walker (FLRW) Metric

The universe is currently based on the Friedmann- Lemaitre-Robertson-Walker (FRW) cosmological model, which sometimes referred to as the hot big bang model. The FLRW model made intelligent speculations in cosmology about the universe as early as 10^{-43} seconds after the Big Bang. According to FLRW CP is valid and forms the basis of the standard model of cosmology. It assumes that our universe is homogeneous and isotropic. Below is the Lemaitre-Robertson-Walker metric.

$$ds^2 = -dt^2 + a^2(t)g_{ij}dx^i dx^j \quad (21)$$

Where g_{ij} will refer to three-dimensional quantities and $i, j = 1, 2, 3$

The relevant components of the Riemann tensor is given by,

$$R_{\mu\nu}^{\alpha} = \partial_{\alpha}\Gamma_{\mu\nu}^{\alpha} - \partial_{\nu}\Gamma_{\mu\alpha}^{\alpha} + \Gamma_{\alpha\beta}^{\alpha}\Gamma_{\mu\nu}^{\beta} - \Gamma_{\beta\nu}^{\alpha}\Gamma_{\mu\alpha}^{\beta} \quad (22)$$

Where $\Gamma_{\mu\nu}^{\alpha}$ is called the Christoffel symbols and it can be calculated in terms of a(t) as follows,

$$\Gamma_{\mu\nu}^{\sigma} = \frac{1}{2} g^{\sigma\beta} (\partial_{\mu} g_{\beta\nu} + \partial_{\nu} g_{\mu\beta} - \partial_{\beta} g_{\mu\nu}) \quad (23)$$

we may compute the Christoffel components,

$$\begin{aligned} \Gamma_{00}^0 &= \Gamma_{00}^i = \Gamma_{i0}^0 = \Gamma_{0i}^0 = 0, & \Gamma_{i0}^i &= \Gamma_{0i}^i = \frac{\dot{a}}{a} \\ \Gamma_{22}^1 &= -r(1 - kr^2) & \Gamma_{33}^2 &= -\sin\theta \cos\theta \\ \Gamma_{33}^1 &= -r(1 - kr^2) \sin^2\theta & \Gamma_{23}^3 &= \Gamma_{32}^3 = \cot\theta \\ \Gamma_{12}^2 &= \Gamma_{21}^2 = \frac{1}{r} & \Gamma_{33}^0 &= a\dot{a}r^2 \sin^2\theta \\ \Gamma_{13}^3 &= \Gamma_{31}^3 = \frac{1}{r} & \Gamma_{22}^0 &= a\dot{a}r^2 \\ \Gamma_{11}^0 &= \frac{a\dot{a}}{1 - kr^2} & \Gamma_{11}^1 &= \frac{kr}{1 - kr^2} \end{aligned} \quad (24)$$

Therefore, for the FLRW metric are, we have

$$\begin{aligned} R_{00} &= -3\frac{\ddot{a}}{a} & R_{11} &= \frac{a\ddot{a} + 2\dot{a}^2 + 2k}{1 - kr^2} \\ R_{22} &= (a\ddot{a} + 2\dot{a}^2 + 2k)r^2 & R_{33} &= (a\ddot{a} + 2\dot{a}^2 + 2k)r^2 \sin^2\theta \end{aligned} \quad (25)$$

Therefore the Ricci Tensor becomes,

$$\begin{aligned} R_{\mu\nu} &= -3\frac{\ddot{a}}{a} + \frac{a\ddot{a} + 2\dot{a}^2 + 2k}{1 - kr^2} + (a\ddot{a} + 2\dot{a}^2 + 2k)r^2 + (a\ddot{a} \\ &\quad + 2\dot{a}^2 + 2k)r^2 \sin^2\theta \end{aligned} \quad (26)$$

The Ricci scalar is written as

$$\begin{aligned} R &= g^{\mu\nu} R_{\mu\nu} = g^{00} R_{00} + g^{11} R_{11} + g^{22} R_{22} + g^{33} R_{33} \\ &= 6\left(\frac{\ddot{a}}{a} + \frac{\dot{a}^2}{a^2} + \frac{k}{a^2}\right) \end{aligned} \quad (27)$$

The Einstein tensor $G_{\mu\nu} = R_{\mu\nu} - \frac{1}{2} g_{\mu\nu} R$ has the components

$$G_{00} = 3\left(\frac{\dot{a}^2 + k}{a^2}\right) \quad G_{0i} = 0$$

$$G_{ij} = -\left(2\frac{\ddot{a}}{a} + \frac{\dot{a}^2}{a^2} + \frac{k}{a^2}\right)g_{ij} \quad (28)$$

Energy momentum tensor describes perfect fluid which FLRW model assumes to be contained in matter. From equation (20) on the right-hand side is the energy-momentum tensor which can be written as shown below and it is for the case of zero observer measure velocity.

$$T^{\mu\nu} = (\rho + p)u^\mu u^\nu - g^{\mu\nu}p \quad (29)$$

$$u^\mu = u_\mu = \begin{pmatrix} 1 \\ 0 \\ 0 \\ 0 \end{pmatrix} \quad (30)$$

$$T_\nu^\mu = \begin{pmatrix} \rho & 0 & 0 & 0 \\ 0 & -p & 0 & 0 \\ 0 & 0 & -p & 0 \\ 0 & 0 & 0 & -p \end{pmatrix} \quad (31)$$

Therefore trace of the FLRW stress energy tensor is

$$T = T_\nu^\mu = \rho - 3p \quad (32)$$

The first Friedmann equation is

$$G_{00} = 8\pi G T_{00} + g_{00}\Lambda \quad (33)$$

$$H^2 = \frac{8\pi G\rho}{3} - \frac{k}{a^2} + \frac{\Lambda}{3}$$

The zero-zero component of trace inverted gives the second Friedmann equation which is called the acceleration equation.

$$\frac{\ddot{a}}{a} = -\frac{4\pi G}{3}(\rho + 3p) + \frac{\Lambda}{3} \quad (34)$$

Where $\frac{\dot{a}}{a} = H$ and $\frac{\ddot{a}}{a} = \dot{H}$

So the second equation can be rewritten as

$$\dot{H} = -\frac{4\pi G}{3}(\rho + 3p) + \frac{\Lambda}{3} \quad (35)$$

The acceleration equation can be obtained by differentiating the first Friedman equation and using the continuity equation.

3.3 Density and Density parameter

The density of the universe provides enough information on the curvature of the universe. This curvature can help us to understand how the universe is evolving. From Eq (26) we can obtain density as follows.

First we rewrite Eq (26) as

$$H^2 = \frac{8\pi G}{3}(\rho_r + \rho_m + \rho_d) - \frac{k}{a^2} + \frac{\Lambda}{3} \quad (36)$$

Where,

$$\rho = \rho_r + \rho_m + \rho_d \quad (37)$$

And the densities depends on time as follows

$$\begin{aligned} \rho_k(t) &= \frac{\rho_{k,0}}{a^4} \\ \rho_\rho(t) &= \frac{\rho_{\rho,0}}{a^3} \\ \rho_\Lambda(t) &= \rho_{\Lambda,0} \end{aligned} \quad (38)$$

These densities are normally expressed in terms of critical density an shown in Equation (39)

$$\rho_c = \frac{3H^2}{4\pi G} \quad (39)$$

In order to make the density ρ dimensionless, we express it as a ratio of ρ_c as shown below

$$\Omega_0 = \frac{\rho}{\rho_c} \quad (40)$$

And the symbol Ω_0 is called density parameter which is the sum of all density parameters from, ρ_r, ρ_m, ρ_d and is given as

$$\Omega_0 = \Omega_\rho + \Omega_k + \Omega_\Lambda \quad (41)$$

3.4 Cosmic Microwave Background (CMB) Radiation

Many probes that study CMB has indicates that thorough this radiations we are able go back in time and explore the universe even when it was only 300,000 years old. It has been established that the cosmic microwave background photons we observe today comes from earliest time back and has been travelling through space which means these radiations scattered off electrons at redshift 1100. Therefore, CMB photons probe gives powerful insight of the early universe. Also, this clearly indicates that the electrons must have been in equilibrium before collisions and hence scattering took place. That is, they should have a blackbody spectrum. The cosmic microwave background (CMB) is the oldest cosmological signal we can currently observe. Mapping its fluctuations gives a wealth of accurate information on processes before, during and after the recombination.

The recent WMAP and Planck satellites have measured several parameters to percent accuracy by comparing the temperature and polarization anisotropies to predictions.

At the young age of the universe, even before the stars and planets could form, it is believed that it was not only denser and hotter but also was filled with a uniform glow from a white-hot hydrogen plasma fog and this plasma together with the radiations got cold due to the expansion of the universe.

The CMB photons were first captured in 1965 by Penzias and Wilson, definitely confirming the hot big bang scenario. As the universe was cooling the protons and electrons were combining to form atoms and this time period at which atoms formed is known as the recombination epoch. It's the time primordial fluctuations created during inflation left their imprint on the photons last scattered at recombination. We also have the time period called photon decoupling, is the time in which photons started to travel through space after. Since CMB radiations are crucial in cosmology its measurement needs to be accurate. One of the

main problems of CMB observations in cosmology is the removal of foregrounds due to various non-cosmological effects.

CHAPTER FOUR: RESEARCH METHODOLOGY

This research work will begin by looking at the Einstein Field Equations (EFE). We will use it in studying the current Λ CDM standard cosmological model, that is, the FLRW model which assumes the Universe to be flat and by extension we will use it to explore the evidence of a possible closed universe as the PL18 suggests. The universe's matter content must be a perfect fluid as a necessary and sufficient condition for spacetime to be FLRW. This means that its velocity field source should have no rotation, shear and acceleration, the second condition is that cold dark energy has to be in the form of a cosmological constant; 'Lambda' Λ . This research will also explore and understand the overall implications of the closed universe to the current and future observations

The packages and programs that will be used in the simulations of the derived equations will include: Python and CAMB. Python is a programming language that integrates systems quickly and more effectively and can be used to plot 2 and 3-dimension graphs of functions, data and data fits, while CAMB is a Fortran 90 application that uses input code to compute CMB spectra by simply inputting cosmological parameters.

4.1.1 Source of Data

We will use data from the Planck's Legacy 2018 for the Evidence of a Closed Universe. Another source will be Archive, a multi-mission that analyses Microwave Background Data (LAMBDA) which is under National Aeronautics and Space Administration (NASA), a cosmic microwave background radiation research expertise center LAMBDA, which aims to serve the CMB research community, and the entire cosmological research community.

4.1.2 Planck, WMAP

Planck is the space mission whose aim is to measure anisotropies in the CMB. It comes third after COBE and WMAP. Planck reported its first cosmological research in a series of papers first 15.5 months of temperature data. However, the report on cosmological parameters constrains was from Planck Collaboration XVI (2014). The WMAP is a NASA Explorer mission.

4.1.3 Data type and Description

We will make use of the following three year CMB data which is freely downloadable from the LAMBDA website; Temperature (TT), Temperature-polarization correlation (TE), Temperature-polarization cross (TB), EE and BB power spectra.

4.1.4 Data Analysis Tools

Analysis of the CMB data will be done using the following tools which are also provided by the LAMBDA.

4.1.4.1 HEALPix (Anafast)

HEALPix which stands for Hierarchical Equal Area isoLatitude Pixelation of a sphere.its able to divide into pixels the spherical surface in which every pixel will have equal surface area.

4.1.4.2 Code for Anisotropies in the Microwave Background (CAMB) and Python in Integration of Differential Equations.

Python - is a programming language that lets you work quickly and integrate systems more effectively. We used OdeInt in Spyder and Jupyter Notebook packages in python, an interface with odeint package used to solve differential equation and plot graphs using matplotlib.pyplot.

The CAMB is an application from Fortran 90 that computes spectra from CMB by inputting cosmological parameters. Antony Lewis and Anthony Challinor came up with this package. This package may be downloadable from <http://camb.info/>. It has a web-based server-side interface users input parameters in a web server form and run the program on it. The results are displayed graphically and the files are downloadable.

4.1.4.3 WMAP Likelihood Software

WMAP team use this software to compute matrices especially those of Fisher and Master. It is also used to compute the FLRW likelihood model. The software is also from Fortran 90 and it has been tested with the SGI MIPSpro, NAG, and Intel FORTRAN 90 compilers.

4.2 The Governing Equations

4.2.1 Einstein Field Equations

Albert Einstein Field Equations relate the total energy content within the universe with its curvature. So according to Einstein, the left hand side of equation (20) dictates matter and energy how to curve spacetime and the right hand side of the equation tells matter and energy how to move through a curved spacetime as introduced in equation (20) in chapter three.

4.2.1.1 Lemaitre-Robertson-Walker metric

For a homogeneous and isotropic universe we use Lemaitre-Robertson-Walker metric as shown in equation (21).

For radial coordinates equation (21) can be rewritten as

$$ds^2 = dt^2 - a^2(t)[dr^2 + \xi^2(r)d\theta^2 + \xi^2(r) \sin^2 \theta d\phi^2] \quad (42)$$

4.2.1.2 Metric tensor

From this metric we obtain the a metric tensor $g_{\mu\nu}$ as shown

$$g_{\mu\nu} = \begin{pmatrix} 1 & 0 & 0 & 0 \\ 0 & -a^2(t) & 0 & 0 \\ 0 & 0 & -a^2(t)\xi^2(r) & 0 \\ 0 & 0 & 0 & -a^2(t)\xi^2(r) \sin^2 \theta \end{pmatrix} \quad (43)$$

To avoid confusion we label the existing radian coordinates as follows.

$$r = \chi \quad (44)$$

Using equation (44) we get

$$g_{\mu\nu} = \begin{pmatrix} 1 & 0 & 0 & 0 \\ 0 & -a^2(t) & 0 & 0 \\ 0 & 0 & -a^2(t)\xi^2(\chi) & 0 \\ 0 & 0 & 0 & -a^2(t)\xi^2(\chi) \sin^2 \theta \end{pmatrix} \quad (45)$$

the equation (45) means that,

$$\begin{aligned} g_{00} &= 1 \\ g_{11} &= -a^2(t) \\ g_{22} &= -a^2(t)\xi^2(\chi) \\ g_{33} &= -a^2(t)\xi^2(\chi) \sin^2 \theta \end{aligned} \quad (46)$$

Otherwise zero.

Therefore, from equation (45) we have

$$\xi^2(\chi) = \begin{cases} \sin^2 \chi & \text{sphere} \\ \chi^2 & \text{flat} \\ \sinh^2 \chi & \text{hperbolic} \end{cases} \quad (47)$$

With this information at hand we can now write the line element of equation (42) as follows

$$ds^2 = dt^2 - a^2(t)[d\chi^2 + \xi^2 d\theta^2 + \xi^2 \sin^2 \theta d\phi^2] \quad (48)$$

The new radial coordinates are as shown below

$$r = \xi(\chi) = \begin{cases} \sin \chi \\ \chi \\ \sinh \chi \end{cases} \quad (49)$$

By differentiating equation (14) and then squaring we get

$$dr^2 = \begin{cases} \cos^2 \chi d\chi^2 \\ d\chi^2 \\ \cosh^2 \chi d\chi^2 \end{cases} \quad (50)$$

From equation (15) we seek to work the initial values of chi so that we complete the variables.

1) For a spherical curvature

$$r = \sin \chi ; dr^2 = \cos^2 \chi d\chi^2$$

$$d\chi^2 = \frac{dr^2}{\cos^2 \chi} = \frac{dr^2}{1-\sin^2 \chi} \quad \text{But for spherical, } r^2 = \sin^2 \chi \text{ therefore,}$$

$$d\chi^2 = \frac{dr^2}{1-r^2} \quad (51)$$

2) For the flat case(non-curved)

$$r = \chi; \quad d\chi^2 = dr^2$$

$$d\chi^2 = \frac{dr^2}{1-0r^2} \quad (52)$$

3) For the hyperbolic curvature (open)

$$r = \sinh \chi ; \text{ and } dr^2 = \cosh^2 \chi d\chi^2$$

$$d\chi^2 = \frac{dr^2}{\cosh^2 \chi} = \frac{dr^2}{1+\sin^2 \chi} \quad \text{but for hyperbolic } r = \sinh \chi \text{ and therefore,}$$

$$d\chi^2 = \frac{dr^2}{1+r^2} \quad (53)$$

From the equations (51), (52) and (53) we can obtain a general equation representing all equations by introducing a constant K which can take three values 1, 0 and -1 as follows;

$$d\chi^2 = \frac{dr^2}{1-k r^2} \quad (54)$$

Where,

$$k = \begin{cases} 1 & \text{for } r = \sin \chi \\ 0 & \text{for } r = \chi \\ -1 & \text{for } r = \sinh \chi \end{cases} \quad (55)$$

Substituting equation (55) in (48) we have a new metric

$$ds^2 = dt^2 - a^2(t) \left[\frac{dr^2}{1 - kr^2} + r^2 d\theta^2 + r^2 \sin^2 \theta d\phi^2 \right] \quad (56)$$

And the metric tensor in equation (45) becomes

$$g_{\mu\nu} = \begin{pmatrix} 1 & 0 & 0 & 0 \\ 0 & \frac{-a^2(t)}{1 - kr^2} & 0 & 0 \\ 0 & 0 & -a^2(t)r^2 & 0 \\ 0 & 0 & 0 & -a^2(t)r^2 \sin^2 \theta \end{pmatrix} \quad (57)$$

4.2.1.3 Ricci tensor and Christoffel symbols

We seek to use this metric to evaluate the Einstein Field Equations (EFE) (20) and find the Friedman field equations. We start with Ricci tensor in equation (22) and the Christoffel symbols given by equation

$$\Gamma_{\mu\nu}^{\sigma} = \frac{1}{2} g^{\sigma\beta} (\partial_{\mu} g_{\beta\nu} + \partial_{\nu} g_{\mu\beta} - \partial_{\beta} g_{\mu\nu})$$

where the metric tensors around it is what we have obtained in equation (63). The μ, σ, ν, β takes value 0,1,2,3 where zero denotes time dimension while 1,2,3 denotes the special dimensions i.e x,y,z. The symbol ∂_{ρ} means a derivative. For $\mu, \sigma, \nu = 0$ we have,

$$\Gamma_{00}^0 = \frac{1}{2} g^{00} (\partial_0 g_{00} + \partial_0 g_{00} - \partial_0 g_{00}) = \frac{1}{2} \left(\frac{\partial 1}{\partial t} + \frac{\partial 1}{\partial t} - \frac{\partial 1}{\partial t} \right) = 0 \quad (58)$$

Also, using the same approach we obtain,

$$\Gamma_{0i}^0 = 0 \quad (59)$$

The non-zero components are as follows

$$\begin{aligned} \Gamma_{11}^0 &= \frac{1}{2} g^{00} (\partial_1 g_{01} + \partial_1 g_{10} - \partial_0 g_{11}) \\ &= -\frac{1}{2} (-\partial_0 g_{11}) \\ &= \frac{1}{2} \frac{\partial}{\partial t} \left(\frac{a^2}{1 - kr^2} \right) \\ &= \frac{a\dot{a}}{1 - kr^2} \end{aligned} \quad (60)$$

$$\begin{aligned}
\Gamma_{22}^0 &= \frac{1}{2} g^{00} (\partial_2 g_{02} + \partial_2 g_{20} - \partial_0 g_{22}) \\
&= -\frac{1}{2} (-\partial_0 g_{22}) \\
&= \frac{1}{2} \frac{\partial}{\partial t} (a^2 r^2) \\
&= a \dot{a} r^2
\end{aligned} \tag{61}$$

$$\begin{aligned}
\Gamma_{33}^0 &= \frac{1}{2} g^{00} (\partial_3 g_{03} + \partial_3 g_{30} - \partial_0 g_{33}) \\
&= -\frac{1}{2} (-\partial_0 g_{33}) \\
&= \frac{1}{2} \frac{\partial}{\partial t} (a^2 r^2 \sin^2 \theta) \\
&= a \dot{a} r^2 \sin^2 \theta
\end{aligned} \tag{62}$$

$$\begin{aligned}
\Gamma_{10}^1 &= \Gamma_{01}^1 = \frac{1}{2} g^{11} (\partial_1 g_{01} + \partial_0 g_{11} - \partial_1 g_{10}) \\
&= \frac{1}{2} g^{11} (\partial_0 g_{11}) \\
&= \frac{1}{2} \left(\frac{1 - kr^2}{-a^2} \right) \frac{\partial}{\partial t} \left(\frac{-a^2}{1 - kr^2} \right) \\
&= \frac{\dot{a}}{a}
\end{aligned} \tag{63}$$

$$\begin{aligned}
\Gamma_{20}^2 &= \Gamma_{02}^2 = \frac{1}{2} g^{22} (\partial_2 g_{02} + \partial_0 g_{22} - \partial_2 g_{20}) \\
&= \frac{1}{2} g^{22} (\partial_0 g_{22}) \\
&= \frac{1}{2} \left(\frac{1}{-a^2 r^2} \right) \frac{\partial}{\partial t} (-a^2 r^2) \\
&= \frac{\dot{a}}{a}
\end{aligned} \tag{64}$$

$$\begin{aligned}
\Gamma_{30}^3 &= \Gamma_{03}^3 = \frac{1}{2} g^{33} (\partial_3 g_{03} + \partial_0 g_{33} - \partial_3 g_{30}) \\
&= \frac{1}{2} g^{33} (\partial_0 g_{33})
\end{aligned} \tag{65}$$

$$\begin{aligned}
&= \frac{1}{2} \left(-\frac{1}{-a^2 r^2 \sin^2 \theta} \right) \frac{\partial}{\partial t} (-a^2 r^2 \sin^2 \theta) \\
&= \frac{\dot{a}}{a}
\end{aligned}$$

$$\begin{aligned}
\Gamma_{33}^1 &= \frac{1}{2} g^{11} (\partial_3 g_{31} + \partial_3 g_{13} - \partial_1 g_{33}) \\
&= \frac{1}{2} g^{11} (-\partial_1 g_{33}) \\
&= -\frac{1}{2} \left(\frac{1 - kr^2}{-a^2} \right) \frac{\partial}{\partial r} (-a^2 r^2 \sin^2 \theta) \\
&= -r(1 - kr^2 \sin^2 \theta)
\end{aligned} \tag{66}$$

$$\begin{aligned}
\Gamma_{22}^1 &= \frac{1}{2} g^{11} (\partial_2 g_{21} + \partial_2 g_{12} - \partial_1 g_{22}) \\
&= \frac{1}{2} g^{11} (-\partial_1 g_{22}) \\
&= -\frac{1}{2} \left(\frac{1 - kr^2}{-a^2} \right) \frac{\partial}{\partial r} (-a^2 r^2) \\
&= -r(1 - kr^2)
\end{aligned} \tag{67}$$

$$\begin{aligned}
\Gamma_{11}^1 &= \frac{1}{2} g^{11} (\partial_1 g_{11} + \partial_1 g_{11} - \partial_1 g_{11}) \\
&= \frac{1}{2} g^{11} (\partial_1 g_{11}) \\
&= -\frac{1}{2} \left(\frac{1 - kr^2}{-a^2} \right) \frac{\partial}{\partial r} \left(\frac{a^2}{1 - kr^2} \right) \\
&= \frac{kr}{1 - kr^2}
\end{aligned} \tag{68}$$

$$\begin{aligned}
\Gamma_{12}^2 = \Gamma_{21}^2 &= \frac{1}{2} g^{22} (\partial_2 g_{12} + \partial_1 g_{22} - \partial_2 g_{21}) \\
&= \frac{1}{2} g^{22} (\partial_1 g_{22}) \\
&= -\frac{1}{2} \left(\frac{1}{-a^2 r^2} \right) \frac{\partial}{\partial r} (a^2 r^2) \\
&= \frac{1}{r}
\end{aligned} \tag{69}$$

$$\begin{aligned}
\Gamma_{33}^2 &= \frac{1}{2} g^{22} (\partial_3 g_{23} + \partial_3 g_{32} - \partial_2 g_{33}) \\
&= \frac{1}{2} g^{22} (-\partial_2 g_{33}) \\
&= -\frac{1}{2} \left(\frac{1}{-a^2 r^2} \right) \frac{\partial}{\partial \theta} (a^2 r^2 \sin^2 \theta) \\
&= -\sin \theta \cos \theta
\end{aligned} \tag{70}$$

$$\begin{aligned}
\Gamma_{23}^3 = \Gamma_{32}^3 &= \frac{1}{2} g^{33} (\partial_2 g_{33} + \partial_3 g_{32} - \partial_3 g_{23}) \\
&= \frac{1}{2} g^{33} (-\partial_2 g_{33}) \\
&= -\frac{1}{2} \left(\frac{1}{a^2 r^2 \sin^2 \theta} \right) \frac{\partial}{\partial \theta} (-a^2 r^2 \sin^2 \theta) \\
&= \cot \theta
\end{aligned} \tag{71}$$

$$\begin{aligned}
\Gamma_{13}^3 = \Gamma_{31}^3 &= \frac{1}{2} g^{33} (\partial_1 g_{33} + \partial_3 g_{31} - \partial_3 g_{13}) \\
&= \frac{1}{2} g^{33} (-\partial_1 g_{33}) \\
&= -\frac{1}{2} \left(\frac{1}{a^2 r^2 \sin^2 \theta} \right) \frac{\partial}{\partial r} (-a^2 r^2 \sin^2 \theta) \\
&= \frac{1}{r}
\end{aligned} \tag{72}$$

With the above computed Criistoffel symbols, we now seek to compute the nonzero Ricci tensor components. We start equation (3)

$$R_{\mu\nu} = \partial_\alpha \Gamma_{\mu\nu}^\alpha - \partial_\nu \Gamma_{\mu\alpha}^\alpha + \Gamma_{\alpha\beta}^\alpha \Gamma_{\mu\nu}^\beta - \Gamma_{\beta\nu}^\alpha \Gamma_{\mu\alpha}^\beta$$

For time-time components

$$\begin{aligned} R_{00} &= \partial_\alpha \Gamma_{00}^\alpha - \partial_0 \Gamma_{0\alpha}^\alpha + \Gamma_{\alpha\beta}^\alpha \Gamma_{00}^\beta - \Gamma_{\beta 0}^\alpha \Gamma_{0\alpha}^\beta \\ &= -\partial_0 \Gamma_{0\alpha}^\alpha - \Gamma_{\beta 0}^\alpha \Gamma_{0\alpha}^\beta \end{aligned} \quad (73)$$

For $\alpha = 0,1,2,3$

$$\begin{aligned} -\partial_0 \Gamma_{0\alpha}^\alpha - \Gamma_{\beta 0}^\alpha \Gamma_{0\alpha}^\beta &= -\partial_0 (\Gamma_{00}^0 + \Gamma_{01}^1 + \Gamma_{02}^2 + \Gamma_{03}^3) - \left(\Gamma_{\beta 0}^0 \Gamma_{00}^\beta + \Gamma_{\beta 0}^1 \Gamma_{01}^\beta + \Gamma_{\beta 0}^2 \Gamma_{02}^\beta + \Gamma_{\beta 0}^3 \Gamma_{03}^\beta \right) \\ &= -\partial_0 (\Gamma_{01}^1 + \Gamma_{02}^2 + \Gamma_{03}^3) - \left(\Gamma_{\beta 0}^1 \Gamma_{01}^\beta + \Gamma_{\beta 0}^2 \Gamma_{02}^\beta + \Gamma_{\beta 0}^3 \Gamma_{03}^\beta \right) \end{aligned}$$

For $\beta = 0,1,2,3$

$$\begin{aligned} &= -\partial_0 (\Gamma_{01}^1 + \Gamma_{02}^2 + \Gamma_{03}^3) - (\Gamma_{00}^1 \Gamma_{01}^0 + \Gamma_{00}^2 \Gamma_{02}^0 + \Gamma_{00}^3 \Gamma_{03}^0 + \Gamma_{10}^1 \Gamma_{01}^1 + \Gamma_{10}^2 \Gamma_{02}^1 + \Gamma_{10}^3 \Gamma_{03}^1 + \Gamma_{20}^1 \Gamma_{01}^2 + \\ &\Gamma_{20}^2 \Gamma_{02}^2 + \Gamma_{20}^3 \Gamma_{03}^2 + \Gamma_{30}^1 \Gamma_{01}^3 + \Gamma_{30}^2 \Gamma_{02}^3 + \Gamma_{30}^3 \Gamma_{03}^3) \\ &= -\partial_0 (\Gamma_{01}^1 + \Gamma_{02}^2 + \Gamma_{03}^3) - (\Gamma_{10}^1 \Gamma_{01}^1 + \Gamma_{20}^2 \Gamma_{02}^2 + \Gamma_{30}^3 \Gamma_{03}^3) \end{aligned}$$

Therefore,

$$\begin{aligned} R_{00} &= -\frac{\partial}{\partial t} \left(\frac{\dot{a}}{a} + \frac{\dot{a}}{a} + \frac{\dot{a}}{a} \right) - \left(\frac{\dot{a}^2}{a^2} + \frac{\dot{a}^2}{a^2} + \frac{\dot{a}^2}{a^2} \right) \\ &= -3 \left(\frac{\ddot{a}a - \dot{a}\dot{a}}{a^2} \right) - 3 \frac{\dot{a}^2}{a^2} \\ &= -3 \frac{\ddot{a}}{a} \end{aligned} \quad (74)$$

For space-space components

$$R_{ij} = \partial_\alpha \Gamma_{ij}^\alpha - \partial_j \Gamma_{i\alpha}^\alpha + \Gamma_{\alpha\beta}^\alpha \Gamma_{ij}^\beta - \Gamma_{\beta j}^\alpha \Gamma_{i\alpha}^\beta \quad (75)$$

For a $i, j = 1$

$$R_{11} = \partial_\alpha \Gamma_{11}^\alpha - \partial_1 \Gamma_{1\alpha}^\alpha + \Gamma_{\alpha\beta}^\alpha \Gamma_{11}^\beta - \Gamma_{\beta 1}^\alpha \Gamma_{1\alpha}^\beta$$

For $\alpha = 0,1,2,3$

$$\begin{aligned} R_{11} &= \partial_0 \Gamma_{11}^0 - \partial_1 \Gamma_{10}^0 + \Gamma_{0\beta}^0 \Gamma_{11}^\beta - \Gamma_{\beta 1}^0 \Gamma_{10}^\beta + \partial_1 \Gamma_{11}^1 - \partial_1 \Gamma_{11}^1 + \Gamma_{1\beta}^1 \Gamma_{11}^\beta - \Gamma_{\beta 1}^1 \Gamma_{11}^\beta + \partial_2 \Gamma_{11}^2 - \partial_1 \Gamma_{12}^2 \\ &\quad + \Gamma_{2\beta}^2 \Gamma_{11}^\beta - \Gamma_{\beta 1}^2 \Gamma_{12}^\beta + \partial_3 \Gamma_{11}^3 - \partial_1 \Gamma_{13}^3 + \Gamma_{3\beta}^3 \Gamma_{11}^\beta - \Gamma_{\beta 1}^3 \Gamma_{13}^\beta \end{aligned}$$

$$= \partial_0 \Gamma_{11}^0 - \Gamma_{\beta 1}^0 \Gamma_{10}^\beta - \partial_1 \Gamma_{12}^2 + \Gamma_{2\beta}^2 \Gamma_{11}^\beta - \Gamma_{\beta 1}^2 \Gamma_{12}^\beta - \partial_1 \Gamma_{13}^3 + \Gamma_{3\beta}^3 \Gamma_{11}^\beta - \Gamma_{\beta 1}^3 \Gamma_{13}^\beta$$

For $\beta = 0, 1, 2, 3$

$$\begin{aligned} &= \partial_0 \Gamma_{11}^0 - \partial_1 \Gamma_{12}^2 - \partial_1 \Gamma_{13}^3 - \Gamma_{01}^0 \Gamma_{10}^0 + \Gamma_{20}^2 \Gamma_{11}^0 - \Gamma_{01}^2 \Gamma_{12}^0 + \Gamma_{30}^3 \Gamma_{11}^0 - \Gamma_{01}^3 \Gamma_{13}^0 - \Gamma_{11}^0 \Gamma_{10}^1 \\ &\quad + \Gamma_{21}^2 \Gamma_{11}^1 - \Gamma_{11}^2 \Gamma_{12}^1 + \Gamma_{31}^3 \Gamma_{11}^1 - \Gamma_{11}^3 \Gamma_{13}^1 - \Gamma_{21}^0 \Gamma_{10}^2 + \Gamma_{22}^2 \Gamma_{11}^2 - \Gamma_{21}^2 \Gamma_{12}^2 + \Gamma_{32}^3 \Gamma_{11}^2 \\ &\quad - \Gamma_{21}^3 \Gamma_{13}^2 - \Gamma_{31}^0 \Gamma_{10}^3 + \Gamma_{23}^2 \Gamma_{11}^3 - \Gamma_{31}^2 \Gamma_{12}^3 + \Gamma_{33}^3 \Gamma_{11}^3 - \Gamma_{31}^3 \Gamma_{13}^3 \\ &= \partial_0 \Gamma_{11}^0 - \partial_1 \Gamma_{12}^2 - \partial_1 \Gamma_{13}^3 + \Gamma_{20}^2 \Gamma_{11}^0 + \Gamma_{30}^3 \Gamma_{11}^0 - \Gamma_{11}^0 \Gamma_{10}^1 + \Gamma_{21}^2 \Gamma_{11}^1 + \Gamma_{31}^3 \Gamma_{11}^1 \\ &= \frac{\partial}{\partial t} \left(\frac{a\dot{a}}{1-kr^2} \right) - \frac{\partial}{\partial r} \frac{1}{r} - \frac{\partial}{\partial r} \frac{1}{r} + \left(\frac{a\dot{a}}{1-kr^2} \right) \frac{\dot{a}}{a} + \left(\frac{a\dot{a}}{1-kr^2} \right) \frac{\dot{a}}{a} - \left(\frac{a\dot{a}}{1-kr^2} \right) \frac{\dot{a}}{a} + \left(\frac{kr}{1-kr^2} \right) \frac{1}{r} \\ &\quad + \left(\frac{kr}{1-kr^2} \right) \frac{1}{r} - \left(\frac{1}{r} \right)^2 - \left(\frac{1}{r} \right)^2 \\ &= \frac{a\ddot{a}}{1-kr^2} + \frac{2\dot{a}^2}{1-kr^2} + \frac{2k}{1-kr^2} \end{aligned}$$

$$R_{11} = \frac{a\ddot{a} + 2\dot{a}^2 + 2k}{1-kr^2} \quad (76)$$

For a $i, j = 2$

$$R_{22} = \partial_\alpha \Gamma_{22}^\alpha - \partial_2 \Gamma_{2\alpha}^\alpha + \Gamma_{\alpha\beta}^\alpha \Gamma_{22}^\beta - \Gamma_{\beta 2}^\alpha \Gamma_{2\alpha}^\beta$$

For $\alpha = 0, 1, 2, 3$

$$\begin{aligned} R_{22} &= \partial_0 \Gamma_{22}^0 - \partial_2 \Gamma_{20}^0 + \Gamma_{0\beta}^0 \Gamma_{22}^\beta - \Gamma_{\beta 2}^0 \Gamma_{20}^\beta + \partial_1 \Gamma_{22}^1 - \partial_2 \Gamma_{21}^1 + \Gamma_{1\beta}^1 \Gamma_{22}^\beta - \Gamma_{\beta 2}^1 \Gamma_{21}^\beta + \partial_2 \Gamma_{22}^2 - \partial_2 \Gamma_{22}^2 \\ &\quad + \Gamma_{2\beta}^2 \Gamma_{22}^\beta - \Gamma_{\beta 2}^2 \Gamma_{22}^\beta + \partial_3 \Gamma_{22}^3 - \partial_2 \Gamma_{23}^3 + \Gamma_{3\beta}^3 \Gamma_{22}^\beta - \Gamma_{\beta 2}^3 \Gamma_{23}^\beta \\ &= \partial_0 \Gamma_{22}^0 + \partial_1 \Gamma_{22}^1 - \Gamma_{\beta 2}^0 \Gamma_{20}^\beta + \Gamma_{1\beta}^1 \Gamma_{22}^\beta - \Gamma_{\beta 2}^1 \Gamma_{21}^\beta + \Gamma_{2\beta}^2 \Gamma_{22}^\beta - \Gamma_{\beta 2}^2 \Gamma_{22}^\beta - \partial_2 \Gamma_{23}^3 + \Gamma_{3\beta}^3 \Gamma_{22}^\beta - \Gamma_{\beta 2}^3 \Gamma_{23}^\beta \end{aligned}$$

For $\beta = 0, 1, 2, 3$

$$\begin{aligned} &= \partial_0 \Gamma_{22}^0 + \partial_1 \Gamma_{22}^1 - \partial_2 \Gamma_{23}^3 - \Gamma_{02}^0 \Gamma_{20}^0 + \Gamma_{10}^1 \Gamma_{22}^0 - \Gamma_{02}^1 \Gamma_{21}^0 + \Gamma_{20}^2 \Gamma_{22}^0 - \Gamma_{02}^2 \Gamma_{22}^0 + \Gamma_{30}^3 \Gamma_{22}^0 - \Gamma_{02}^3 \Gamma_{23}^0 \\ &\quad - \Gamma_{21}^0 \Gamma_{20}^1 + \Gamma_{11}^1 \Gamma_{22}^1 - \Gamma_{12}^1 \Gamma_{21}^1 + \Gamma_{21}^2 \Gamma_{22}^1 - \Gamma_{12}^2 \Gamma_{22}^1 + \Gamma_{31}^3 \Gamma_{22}^1 - \Gamma_{12}^3 \Gamma_{23}^1 - \Gamma_{22}^0 \Gamma_{20}^2 \\ &\quad + \Gamma_{12}^1 \Gamma_{22}^2 - \Gamma_{22}^1 \Gamma_{21}^2 + \Gamma_{22}^2 \Gamma_{22}^2 - \Gamma_{22}^2 \Gamma_{22}^2 + \Gamma_{32}^3 \Gamma_{22}^2 - \Gamma_{22}^3 \Gamma_{23}^2 - \Gamma_{32}^0 \Gamma_{20}^3 + \Gamma_{13}^1 \Gamma_{22}^3 \\ &\quad - \Gamma_{32}^1 \Gamma_{21}^3 + \Gamma_{23}^2 \Gamma_{22}^3 - \Gamma_{32}^2 \Gamma_{22}^3 + \Gamma_{33}^3 \Gamma_{22}^3 - \Gamma_{32}^3 \Gamma_{23}^3 \\ &= \partial_0 \Gamma_{22}^0 + \partial_1 \Gamma_{22}^1 - \partial_2 \Gamma_{23}^3 + \Gamma_{10}^1 \Gamma_{22}^0 + \Gamma_{30}^3 \Gamma_{22}^0 + \Gamma_{11}^1 \Gamma_{22}^1 + \Gamma_{31}^3 \Gamma_{22}^1 - \Gamma_{22}^0 \Gamma_{20}^2 - \Gamma_{22}^1 \Gamma_{21}^2 - \Gamma_{32}^3 \Gamma_{23}^3 \\ &= \frac{\partial}{\partial t} (a\dot{a}r^2) + \frac{\partial}{\partial r} (-r(1-kr^2)) - \frac{\partial}{\partial \theta} \cot \theta + (a\dot{a}r^2) \frac{\dot{a}}{a} + (a\dot{a}r^2) \frac{\dot{a}}{a} \\ &\quad - -r(1-kr^2) \left(\frac{kr}{1-kr^2} \right) - r(1-kr^2) \frac{1}{r} - (a\dot{a}r^2) \frac{\dot{a}}{a} + r(1-kr^2) \frac{1}{r} \\ &\quad - \cot^2 \theta \\ &= r^2(a\ddot{a} + 2\dot{a}^2 + 2k) - 1 + \csc^2 \theta - \cot^2 \theta \end{aligned}$$

$$= r^2(a\ddot{a} + 2\dot{a}^2 + 2k) \quad (77)$$

For a $i, j = 3$

$$R_{33} = \partial_\alpha \Gamma_{33}^\alpha - \partial_3 \Gamma_{3\alpha}^\alpha + \Gamma_{\alpha\beta}^\alpha \Gamma_{33}^\beta - \Gamma_{\beta 3}^\alpha \Gamma_{3\alpha}^\beta$$

For $\alpha = 0, 1, 2, 3$

$$\begin{aligned} &= \partial_0 \Gamma_{33}^0 - \partial_3 \Gamma_{30}^0 + \Gamma_{0\beta}^0 \Gamma_{33}^\beta - \Gamma_{\beta 3}^0 \Gamma_{30}^\beta + \partial_1 \Gamma_{33}^1 - \partial_3 \Gamma_{31}^1 + \Gamma_{1\beta}^1 \Gamma_{33}^\beta - \Gamma_{\beta 3}^1 \Gamma_{31}^\beta + \partial_2 \Gamma_{33}^2 - \partial_3 \Gamma_{32}^2 \\ &\quad + \Gamma_{2\beta}^2 \Gamma_{33}^\beta - \Gamma_{\beta 3}^2 \Gamma_{32}^\beta + \partial_3 \Gamma_{33}^3 - \partial_3 \Gamma_{33}^3 + \Gamma_{3\beta}^3 \Gamma_{33}^\beta - \Gamma_{\beta 3}^3 \Gamma_{33}^\beta \\ &= \partial_0 \Gamma_{33}^0 + \partial_1 \Gamma_{33}^1 + \partial_2 \Gamma_{33}^2 - \Gamma_{\beta 3}^0 \Gamma_{30}^\beta + \Gamma_{1\beta}^1 \Gamma_{33}^\beta - \Gamma_{\beta 3}^1 \Gamma_{31}^\beta + \Gamma_{2\beta}^2 \Gamma_{33}^\beta - \Gamma_{\beta 3}^2 \Gamma_{32}^\beta + \Gamma_{3\beta}^3 \Gamma_{33}^\beta - \Gamma_{\beta 3}^3 \Gamma_{33}^\beta \end{aligned}$$

For $\beta = 0, 1, 2, 3$

$$\begin{aligned} &= \partial_0 \Gamma_{33}^0 + \partial_1 \Gamma_{33}^1 + \partial_2 \Gamma_{33}^2 - \Gamma_{03}^0 \Gamma_{30}^0 + \Gamma_{10}^1 \Gamma_{33}^0 - \Gamma_{03}^1 \Gamma_{31}^0 + \Gamma_{20}^2 \Gamma_{33}^0 - \Gamma_{03}^2 \Gamma_{32}^0 + \Gamma_{30}^3 \Gamma_{33}^0 - \Gamma_{03}^3 \Gamma_{33}^0 \\ &\quad - \Gamma_{13}^0 \Gamma_{30}^1 + \Gamma_{11}^1 \Gamma_{33}^1 - \Gamma_{13}^1 \Gamma_{31}^1 + \Gamma_{21}^2 \Gamma_{33}^1 - \Gamma_{13}^2 \Gamma_{32}^1 + \Gamma_{31}^3 \Gamma_{33}^1 - \Gamma_{13}^3 \Gamma_{33}^1 - \Gamma_{23}^0 \Gamma_{30}^2 \\ &\quad + \Gamma_{12}^1 \Gamma_{33}^2 - \Gamma_{23}^1 \Gamma_{31}^2 + \Gamma_{22}^2 \Gamma_{33}^2 - \Gamma_{23}^2 \Gamma_{32}^2 + \Gamma_{32}^3 \Gamma_{33}^2 - \Gamma_{23}^3 \Gamma_{33}^2 - \Gamma_{33}^0 \Gamma_{30}^3 + \Gamma_{13}^1 \Gamma_{33}^3 \\ &\quad - \Gamma_{33}^1 \Gamma_{31}^3 + \Gamma_{23}^2 \Gamma_{33}^3 - \Gamma_{33}^2 \Gamma_{32}^3 + \Gamma_{33}^3 \Gamma_{33}^3 - \Gamma_{33}^3 \Gamma_{33}^3 \end{aligned}$$

$$= \partial_0 \Gamma_{33}^0 + \partial_1 \Gamma_{33}^1 + \partial_2 \Gamma_{33}^2 + \Gamma_{10}^1 \Gamma_{33}^0 + \Gamma_{20}^2 \Gamma_{33}^0 + \Gamma_{11}^1 \Gamma_{33}^1 + \Gamma_{21}^2 \Gamma_{33}^1 - \Gamma_{33}^0 \Gamma_{30}^3 - \Gamma_{33}^1 \Gamma_{31}^3 - \Gamma_{33}^2 \Gamma_{32}^3$$

$$\begin{aligned} &= \frac{\partial}{\partial t} (a\dot{a}r^2 \sin^2 \theta) + \frac{\partial}{\partial r} (-r(1 - kr^2) \sin^2 \theta) - \frac{\partial}{\partial \theta} (\sin \theta \cos \theta) + (a\dot{a}r^2 \sin^2 \theta) \frac{\dot{a}}{a} \\ &\quad + (a\dot{a}r^2 \sin^2 \theta) \frac{\dot{a}}{a} - r(1 - kr^2) \sin^2 \theta \left(\frac{kr}{1 - kr^2} \right) - r(1 - kr^2) \sin^2 \theta \frac{1}{r} \\ &\quad - (a\dot{a}r^2 \sin^2 \theta) \frac{\dot{a}}{a} + r(1 - kr^2) \sin^2 \theta \frac{1}{r} + \cot \theta \sin \theta \cos \theta \end{aligned}$$

$$\begin{aligned} &= r^2 \sin^2 \theta (a\ddot{a} + \dot{a}^2) - \sin^2 \theta (1 - 3kr^2) + \sin^2 \theta \\ &\quad - \cos^2 \theta + \dot{a}^2 r^2 \sin^2 \theta - \sin^2 \theta kr^2 + \cos^2 \theta \end{aligned}$$

$$= r^2 \sin^2 \theta (a\ddot{a} + \dot{a}^2) + \sin^2 \theta 2kr^2 + \dot{a}^2 r^2 \sin^2 \theta$$

$$R_{33} = (a\ddot{a} + 2\dot{a}^2 + 2k)r^2 \sin^2 \theta \quad (78)$$

Therefore,

$$R_{\mu\nu} = R_{00} + R_{11} + R_{22} + R_{33}$$

$$= -3\frac{\ddot{a}}{a} + \frac{a\ddot{a} + 2\dot{a}^2 2k}{1 - kr^2} + r^2(a\ddot{a} + 2\dot{a}^2 + 2k) + (a\ddot{a} + 2\dot{a}^2 + 2k)r^2 \sin^2 \theta \quad (79)$$

4.2.1.4 Ricci scalar

Having calculated the Ricci tensor, we seek to calculate the Ricci scalar as shown

$$R = g^{\mu\nu} R_{\mu\nu} = g^{00} R_{00} + g^{11} R_{11} + g^{22} R_{22} + g^{33} R_{33}$$

We can write the Ricci tensor as a metric tensor as follows

$$R_{\mu\nu} = \begin{pmatrix} -3\frac{\ddot{a}}{a} & 0 & 0 & 0 \\ 0 & \frac{a\ddot{a} + 2\dot{a}^2 2k}{1 - kr^2} & 0 & 0 \\ 0 & 0 & r^2(a\ddot{a} + 2\dot{a}^2 + 2k) & 0 \\ 0 & 0 & 0 & (a\ddot{a} + 2\dot{a}^2 + 2k)r^2 \sin^2 \theta \end{pmatrix} \quad (80)$$

And remember the metric tensor

$$g_{\mu\nu} = \begin{pmatrix} 1 & 0 & 0 & 0 \\ 0 & -a^2(t) & 0 & 0 \\ 0 & 0 & -a^2(t)r^2 & 0 \\ 0 & 0 & 0 & -a^2(t)r^2 \sin^2 \theta \end{pmatrix}$$

Therefore, the Ricci scalar becomes

$$R =$$

$$\begin{aligned} & -3\frac{\ddot{a}}{a} - \frac{1-kr^2}{a^2(t)} \left(\frac{a\ddot{a} + 2\dot{a}^2 2k}{1-kr^2} \right) - r^2(a\ddot{a} + 2\dot{a}^2 + 2k) \frac{1}{-a^2(t)r^2} - \\ & (a\ddot{a} + 2\dot{a}^2 + 2k)r^2 \sin^2 \theta \frac{1}{-a^2(t)r^2 \sin^2 \theta} \\ & = -3\frac{\ddot{a}}{a} - 3 \left(\frac{a\ddot{a} + 2\dot{a}^2 + 2k}{a^2} \right) \\ & = -6 \left(\frac{\ddot{a}}{a} + \frac{\dot{a}^2}{a^2} + \frac{k}{a^2} \right) \end{aligned} \quad (81)$$

4.2.1.5 Einstein tensor components

Now we can calculate the zero-zero Einstein tensor component.

Given the equation

$$G_{\mu\nu} = R_{\mu\nu} - \frac{1}{2} g_{\mu\nu} R$$

For $\mu, \nu = 0$

$$G_{00} = R_{00} - \frac{1}{2}g_{00}R = -3\frac{\ddot{a}}{a} + \frac{1}{2}6\left(\frac{\ddot{a}}{a} + \frac{\dot{a}^2}{a^2} + \frac{k}{a^2}\right)$$

$$G_{00} = 3\left(\frac{\dot{a}^2 + k}{a^2}\right) \quad (82)$$

Also the zero-zero Einstein tensor can be written as

$$G_{00} = 8\pi GT_{00}$$

4.2.1.6 Energy momentum tensor

To work out necessary pieces from the stress energy momentum tensor, we employ the stress energy momentum tensor for a perfect fluid for the case of zero observer measure velocity.

$$T^{\mu\nu} = (\rho + p)u^\mu u^\nu - g^{\mu\nu}p \quad (83)$$

Where

$$u^\mu = u_\mu = \begin{pmatrix} 1 \\ 0 \\ 0 \\ 0 \end{pmatrix} \text{ is the velocity.}$$

$$T_\nu^\mu = g_{\nu\alpha}T^{\mu\alpha} = (\rho + p)u^\mu u^\alpha g_{\nu\alpha} - g_{\nu\alpha}g^{\mu\alpha}p$$

$$= (\rho + p)u^\mu u_\nu - \delta_\nu^\mu p$$

Also

$$T_{\mu\nu} = g_{\mu\alpha}T_\nu^\alpha = (\rho + p)u^\alpha u_\nu g_{\mu\alpha} - g_{\mu\nu}p$$

$$T_{\mu\nu} = (\rho + p)u_\mu u_\nu - g_{\mu\nu}p$$

$$T_\nu^\mu = (\rho + p) \begin{pmatrix} 1 \\ 0 \\ 0 \\ 0 \end{pmatrix} \begin{pmatrix} 1 \\ 0 \\ 0 \\ 0 \end{pmatrix} - \begin{pmatrix} 1 & 0 & 0 & 0 \\ 0 & 1 & 0 & 0 \\ 0 & 0 & 1 & 0 \\ 0 & 0 & 0 & 1 \end{pmatrix} p = \begin{pmatrix} \rho + p & 0 & 0 & 0 \\ 0 & 0 & 0 & 0 \\ 0 & 0 & 0 & 0 \\ 0 & 0 & 0 & 0 \end{pmatrix} - \begin{pmatrix} p & 0 & 0 & 0 \\ 0 & p & 0 & 0 \\ 0 & 0 & p & 0 \\ 0 & 0 & 0 & p \end{pmatrix}$$

$$T_\nu^\mu = \begin{pmatrix} \rho & 0 & 0 & 0 \\ 0 & -p & 0 & 0 \\ 0 & 0 & -p & 0 \\ 0 & 0 & 0 & -p \end{pmatrix} \quad (84)$$

Therefore, the trace of the RLRW stress energy tensor is

$$T = T_v^\mu = \rho - 3p$$

Hence,

$$T_{00} = \rho \tag{85}$$

Given the zero-zero Einstein tensor equation as

$$G_{00} = 8\pi GT_{00}$$

4.2.1.7 First Friedmann Equation

By substituting equations (81) and (82) we obtain the Friedman equation

$$3\left(\frac{\dot{a}^2 + k}{a^2}\right) = 8\pi G\rho$$

At this stage we can introduce the Cosmological constant Lambda (Λ), we have

$$3\left(\frac{\dot{a}^2 + k}{a^2}\right) = 8\pi G\rho + \Lambda$$

This equation can be written as

$$3\left(\frac{\dot{a}^2}{a^2} + \frac{k}{a^2}\right) = 8\pi G\rho + \Lambda$$

We let $\frac{\dot{a}}{a} = H$ a value known as the Hubble constant. Therefore, we have

$$3\left(H^2 + \frac{k}{a^2}\right) = 8\pi G\rho + \Lambda$$

Hence

$$H^2 = \frac{8\pi G\rho}{3} - \frac{k}{a^2} + \frac{\Lambda}{3} \tag{86}$$

Equation (86) is called the first Friedmann Equation.

4.2.1.8 Second Friedmann Equation

To calculate the second Friedmann equation, we invert the zero-zero traced FLRW as follows.

$$R_{\mu\nu} - \frac{1}{2}g_{\mu\nu}R = 8\pi GT_{\mu\nu} + g_{\mu\nu}\Lambda$$

By inverting we multiply through by $g^{\mu\nu}$ and we get

$$\begin{aligned} R - \frac{D}{2}R &= 8\pi GT + \Lambda D \\ &= \frac{8\pi GT + \Lambda D}{1 - \frac{D}{2}} \end{aligned}$$

$$R = -8\pi GT - 4\Lambda$$

Multiply both sides by $-\frac{1}{2}g_{\mu\nu}$

$$-\frac{1}{2}g_{\mu\nu}R = \frac{1}{2}g_{\mu\nu}8\pi GT + 2g_{\mu\nu}\Lambda$$

Now let's subtract the EFE in both sides

$$-\frac{1}{2}g_{\mu\nu}R - \left(R_{\mu\nu} - \frac{1}{2}g_{\mu\nu}R\right) = \frac{1}{2}g_{\mu\nu}8\pi GT + 2g_{\mu\nu}\Lambda - (8\pi GT_{\mu\nu} + g_{\mu\nu}\Lambda)$$

$$R_{\mu\nu} = 8\pi G \left(T_{\mu\nu} - \frac{1}{2}Tg_{\mu\nu}\right) - g_{\mu\nu}\Lambda \quad (87)$$

The zero-zero component become

$$R_{00} = 8\pi G \left(T_{00} - \frac{1}{2}Tg_{00}\right) - g_{00}\Lambda$$

$$-3\frac{\ddot{a}}{a} = 8\pi G \left(\rho - \frac{1}{2}(\rho + 3p)\right) - \Lambda$$

$$\frac{\ddot{a}}{a} = -\frac{4\pi G}{3}(\rho + 3p) + \frac{\Lambda}{3} \quad (88)$$

Equation (88) is the second Friedmann equation.

4.2.1.9 Raychaudhuri equation

We can obtain the Einstein tensor spatial non zero components as follows

$$G_{ij} = R_{ij} - \frac{1}{2}g_{ij}R = 8\pi GT_{ij} + g_{ij}\Lambda$$

$$R_{ij} - \frac{1}{2}g_{ij}R = 8\pi GT_{ij} + g_{ij}\Lambda$$

(89)

We substitute the values of R_{ij} from equation (44), R from eq (46) and the metric tensor g_{ij} with only spatial components as shown below

$$\begin{aligned}
& \frac{a\ddot{a}+2\dot{a}^2+2k}{1-kr^2} + r^2(a\ddot{a} + 2\dot{a}^2 + 2k) + \\
& (a\ddot{a} + 2\dot{a}^2 + 2k)r^2 \sin^2 \theta - \frac{1}{2} \left(\frac{-a^2(t)}{1-kr^2} - a^2(t)r^2 - a^2(t)r^2 \sin^2 \theta \right) \left(-6 \left(\frac{\ddot{a}}{a} + \frac{\dot{a}^2}{a^2} + \frac{k}{a^2} \right) \right) = \\
& 8\pi G T_{ij} + \left(\frac{-a^2(t)}{1-kr^2} - a^2(t)r^2 - a^2(t)r^2 \sin^2 \theta \right) \Lambda \\
& \left(\frac{1}{1-kr^2} + r^2 + r^2 \sin^2 \theta \right) (a\ddot{a} + 2\dot{a}^2 + 2k) - \frac{-a^2(t)}{2} \left(\frac{1}{1-kr^2} + r^2 + r^2 \sin^2 \theta \right) \left(-6 \left(\frac{\ddot{a}}{a} + \frac{\dot{a}^2}{a^2} + \frac{k}{a^2} \right) \right) = 8\pi G T_{ij} + \frac{-a^2(t)}{2} \left(\frac{1}{1-kr^2} + r^2 + r^2 \sin^2 \theta \right) \Lambda
\end{aligned}$$

Dividing both sides with $\frac{a^2(t)}{2} \left(\frac{1}{1-kr^2} + r^2 + r^2 \sin^2 \theta \right) = g_{ij}$ (remember $\frac{1}{g_{ij}} = g^{ij}$) and we have

$$\left(\frac{a\ddot{a}+2\dot{a}^2+2k}{a^2(t)} \right) - 3 \left(\frac{\ddot{a}}{a} + \frac{\dot{a}^2}{a^2} + \frac{k}{a^2} \right) = 8\pi G g^{ij} T_{ij} + \Lambda$$

Letting like terms together and solving we get

$$-\frac{2\ddot{a}}{a} - \frac{\dot{a}^2}{a^2} - \frac{k}{a^2} = 8\pi G g^{ij} T_{ij} + \Lambda$$

$$\frac{-2\ddot{a}}{a} - \frac{\dot{a}^2}{a^2} - \frac{k}{a^2} - \Lambda = 8\pi G g^{ij} T_{ij}$$

$$\frac{2\ddot{a}}{a} + \frac{\dot{a}^2}{a^2} + \frac{k}{a^2} + \Lambda = -8\pi G g^{ij} T_{ij}$$

We can write the value of

$$g^{ij} T_{ij} = g^{\mu\nu} T_{\mu\nu} - g^{00} T_{00} = -3p$$

Therefore, we obtain

$$\frac{2\ddot{a}}{a} + H^2 + \frac{k}{a^2} + \Lambda = 24\pi G P \tag{90}$$

Equation (90) is called the Raychaudhuri equation

4.2.2 Energy-Momentum Conservation

For the conservation of energy and momentum of the universe we use the relation in Bianchi Identity which is

$$\nabla_{\mu} G^{\mu\nu} = 0 \tag{91}$$

Therefore, to calculate the conservation of energy momentum tensor means to find its derivative and equate to zero as follows.

$$\nabla_{\mu} T^{\mu\nu} = 0 \quad (92)$$

$$\begin{aligned} \nabla_{\mu} T^{\mu\nu} &= \partial_{\mu} T^{\mu\nu} + \Gamma_{\mu\alpha}^{\mu} T^{\alpha\nu} + \Gamma_{\mu\alpha}^{\nu} T^{\mu\alpha} \\ &= \partial_{\mu} g^{\mu\beta} T_{\beta}^{\nu} + \Gamma_{\mu\alpha}^{\mu} g^{\alpha\sigma} T_{\sigma}^{\nu} + \Gamma_{\mu\alpha}^{\nu} g^{\tau\mu} T_{\tau}^{\alpha} \end{aligned} \quad (93)$$

4.2.2.1 Energy conservation

When $\nu = 0$ then we have

$$= \partial_{\mu} g^{\mu\beta} T_{\beta}^0 + \Gamma_{\mu\alpha}^{\mu} g^{\alpha\sigma} T_{\sigma}^0 + \Gamma_{\mu\alpha}^0 g^{\tau\mu} T_{\tau}^{\alpha} \quad (94)$$

when $\mu = 0$, the 2nd and 3rd terms of equation (94) vanishes and the 1st term remains iff $\beta = 0$ as follows

$$\begin{aligned} &= \partial_0 g^{00} T_0^0 + \Gamma_{00}^0 g^{0\sigma} T_{\sigma}^0 + \Gamma_{00}^0 g^{\tau 0} T_{\tau}^0 \\ &\quad \partial_0 g^{00} T_0^0 = \dot{\rho} \end{aligned} \quad (95)$$

When $\mu = i = 1,2,3$, and $\alpha = \sigma = 0$ the 3rd term of eq (95) vanishes and the 2nd term gives

$$\begin{aligned} \Gamma_{\mu 0}^{\mu} g^{00} T_0^0 &= \Gamma_{10}^1 g^{00} T_0^0 + \Gamma_{20}^2 g^{00} T_0^0 + \Gamma_{30}^3 g^{00} T_0^0 \\ &= \frac{\dot{\rho}}{a} + \frac{\dot{\rho}}{a} + \frac{\dot{\rho}}{a} \\ &= 3 \frac{\dot{\rho}}{a} \end{aligned} \quad (96)$$

When $\mu = \alpha = \tau = i = 1,2,3$, the 3rd term gives

$$\begin{aligned} \Gamma_{\mu\alpha}^0 g^{\tau\mu} T_{\tau}^{\alpha} &= \Gamma_{11}^0 g^{11} T_1^1 + \Gamma_{22}^0 g^{22} T_2^2 + \Gamma_{33}^0 g^{33} T_3^3 \\ &= -\frac{\dot{a}a}{1-kr^2} \frac{1-kr^2}{a^2} (-P) - \dot{a}ar^2 \frac{1}{a^2 r^2} (-P) - \dot{a}ar^2 \sin^2 \theta \frac{1}{a^2 r^2 \sin^2 \theta} (-P) \\ &= 3 \frac{\dot{a}}{a} P \end{aligned} \quad (97)$$

Combining equations (95), (96) and (97) equation (94) becomes

$$= \dot{\rho} + 3\frac{\dot{a}}{a}\rho + 3\frac{\dot{a}}{a}P$$

Therefore, the conservation of energy momentum tensor becomes,

$$\begin{aligned}\nabla_{\mu}T^{\mu 0} &= \dot{\rho} + 3H(\rho + P) = 0 \\ \dot{\rho} + 3H(\rho + P) &= 0\end{aligned}\tag{98}$$

Equation (98) is also known as continuity equation.

4.2.2.2 Momentum conservation

When $v = i = 1,2,3$ then we have

$$\begin{aligned}\nabla_{\mu}T^{\mu i} &= \partial_{\mu}g^{\mu\beta}T_{\beta}^i + \Gamma_{\mu\alpha}^{\mu}g^{\alpha\sigma}T_{\sigma}^i + \Gamma_{\mu\alpha}^i g^{\tau\mu}T_{\tau}^{\alpha} \\ &= \partial_{\mu}g^{\mu\beta}T_{\beta}^1 + \Gamma_{\mu\alpha}^{\mu}g^{\alpha\sigma}T_{\sigma}^1 + \Gamma_{\mu\alpha}^1 g^{\tau\mu}T_{\tau}^{\alpha} + \partial_{\mu}g^{\mu\beta}T_{\beta}^2 + \Gamma_{\mu\alpha}^{\mu}g^{\alpha\sigma}T_{\sigma}^2 + \Gamma_{\mu\alpha}^2 g^{\tau\mu}T_{\tau}^{\alpha} \\ &\quad + \partial_{\mu}g^{\mu\beta}T_{\beta}^3 + \Gamma_{\mu\alpha}^{\mu}g^{\alpha\sigma}T_{\sigma}^3 + \Gamma_{\mu\alpha}^3 g^{\tau\mu}T_{\tau}^{\alpha}\end{aligned}$$

For the first term when $u = 1,2,3$ then,

$$\begin{aligned}\partial_{\mu}g^{\mu\beta}T_{\beta}^1 + \Gamma_{\mu\alpha}^{\mu}g^{\alpha\sigma}T_{\sigma}^1 + \Gamma_{\mu\alpha}^1 g^{\tau\mu}T_{\tau}^{\alpha} \\ &= \partial_1 g^{11}T_1^1 + \Gamma_{11}^1 g^{11}T_1^1 + \Gamma_{11}^1 g^{11}T_1^1 + \partial_2 g^{21}T_1^1 + \Gamma_{21}^2 g^{11}T_1^1 + \Gamma_{22}^1 g^{22}T_2^2 \\ &\quad + \partial_3 g^{31}T_1^1 + \Gamma_{31}^3 g^{11}T_1^1 + \Gamma_{33}^1 g^{33}T_3^3 \\ &= \partial_r \left(\frac{1 - k r^2}{a^2} P \right) + \frac{kr}{1 - k r^2} \left(\frac{1 - k r^2}{a^2} P \right) + \frac{kr}{1 - k r^2} \left(\frac{1 - k r^2}{a^2} P \right) + \frac{1}{r} \left(\frac{1 - k r^2}{a^2} P \right) \\ &\quad - \frac{r(1 - k r^2)}{a^2 r^2} P + \frac{1}{r} \left(\frac{1 - k r^2}{a^2} P \right) - \frac{r(1 - k r^2) \sin^2 \theta}{a^2 r^2 \sin^2 \theta} P \\ &= \frac{-2kr}{a^2} P + \frac{kr}{a^2} P + \frac{kr}{a^2} P + \frac{2}{r} \left(\frac{1 - k r^2}{a^2} P \right) - \frac{2}{r} \left(\frac{1 - k r^2}{a^2} P \right) = 0\end{aligned}$$

For the second term when $u = 1,2,3$ we have,

$$\begin{aligned}\partial_{\mu}g^{\mu\beta}T_{\beta}^2 + \Gamma_{\mu\alpha}^{\mu}g^{\alpha\sigma}T_{\sigma}^2 + \Gamma_{\mu\alpha}^2 g^{\tau\mu}T_{\tau}^{\alpha} &= \partial_1 g^{12}T_2^2 + \Gamma_{12}^1 g^{22}T_2^2 + \Gamma_{11}^2 g^{11}T_1^1 + \partial_2 g^{22}T_2^2 + \\ \Gamma_{22}^2 g^{22}T_2^2 + \Gamma_{22}^2 g^{22}T_2^2 + \partial_3 g^{32}T_2^2 + \Gamma_{32}^3 g^{22}T_2^2 + \Gamma_{33}^2 g^{33}T_3^3 \\ &\quad \frac{\cot \theta}{a^2 r^2} P - \frac{\sin \theta \cos \theta}{a^2 r^2 \sin^2 \theta} P = 0\end{aligned}$$

For the third term when $u = 1,2,3$ we have

$$\begin{aligned}\partial_{\mu}g^{\mu\beta}T_{\beta}^3 + \Gamma_{\mu\alpha}^{\mu}g^{\alpha\sigma}T_{\sigma}^3 + \Gamma_{\mu\alpha}^3 g^{\tau\mu}T_{\tau}^{\alpha} &= \partial_1 g^{13}T_3^3 + \Gamma_{13}^1 g^{33}T_3^3 + \Gamma_{11}^3 g^{11}T_1^1 + \partial_2 g^{23}T_3^3 + \\ \Gamma_{23}^2 g^{33}T_3^3 + \Gamma_{22}^3 g^{22}T_2^2 + \partial_3 g^{33}T_3^3 + \Gamma_{33}^3 g^{33}T_3^3 + \Gamma_{33}^3 g^{33}T_3^3 \\ &= \frac{kr}{1 - k r^2} \left(\frac{1}{a^2 r^2 \sin^2 \theta} P \right)\end{aligned}$$

4.2.3 Matter density And Density Parameter

4.2.3.1 Critical density

The critical density can be explained as density in which the universe would halt its expansion which is only after an infinite time.

From the first Friedmann equation (86), the matter density of the universe ρ , by setting the normalized spatial curvature $k = 0$ and assuming Λ to be zero is called the critical density denoted by ρ_c and is given in the form

$$\rho_c = \frac{3H^2}{8\pi G} \quad (99)$$

The first Friedman equation from eq (86)

$$H^2 = \frac{8\pi G\rho}{3} - \frac{k}{a^2} + \frac{\Lambda}{3}$$

Dividing both sides by H^2 we have

$$1 = \frac{8\pi G\rho}{3H^2} - \frac{k}{a^2H^2} + \frac{\Lambda}{3H^2} \quad (100)$$

The first term of eq (100), using eq (99) becomes

$$\frac{8\pi G\rho}{3H^2} = \frac{\rho}{\rho_c} \quad (101)$$

The ρ denotes the matter density of the universe which is the sum of normal matter, baryonic matter, and dark matter gives in the form,

$$\rho = \rho_n + \rho_d + \rho_r = \rho_m + \rho_r \quad (102)$$

The ratio $\frac{\rho}{\rho_c}$ is called the density matter parameter denoted by Ω_m . We express it as a ratio so that its value is dimensionless.

$$\Omega_m = \frac{8\pi G\rho}{3H^2} = \frac{\rho_m}{\rho_c} \quad (103)$$

Similarly, from eq (100) we can have Energy density parameter and cosmological density parameter as follows

$$\Omega_k = -\frac{k}{a^2 H^2} = \frac{\rho_k}{\rho_c}$$

Here, the energy density is given by

$$\rho_k = -\frac{3k}{8\pi G a^2} \quad (104)$$

And for cosmological density parameter we have

$$\Omega_\Lambda = \frac{\Lambda}{3H^2} = \frac{\rho_\Lambda}{\rho_c}$$

Therefore, the cosmological density is

$$\rho_\Lambda = \frac{\Lambda}{8\pi G} \quad (105)$$

Now we can write equation (100) in the form

$$1 = \Omega_m + \Omega_k + \Omega_\Lambda \quad (106)$$

The matter density, critical density, scale factor, density parameters and Hubble constant are all time dependent and we can express them as of now.

The matter density, radiation density and vacuum density as of now are given by

$$\rho_m = \frac{\rho_{m,0}}{a^3}, \quad \rho_r = \frac{\rho_{r,0}}{a^4}, \quad \rho_{\Lambda,0} = \text{constant} \quad (107)$$

And the critical density today, can be written as

$$\rho_{c,0} = \frac{3H_0^2}{8\pi G} \quad (108)$$

From first Friedman equation, assuming $\Lambda = 0$ we can calculate the value of the curvature as follows

$$H_0^2 = \frac{8\pi G \rho_0}{3} - \frac{k}{a^2}$$

Dividing both sides by H_0^2 and noting that $a_0^2 = 1$

$$\begin{aligned}
 1 &= \frac{8\pi G\rho_0}{3H_0^2} - \frac{k}{H_0^2 a_0^2} \\
 1 &= \Omega_0 - \frac{k}{H_0^2} \\
 k &= H_0^2(\Omega_0 - 1)
 \end{aligned} \tag{109}$$

Substituting k back we get

$$H^2 = \frac{8\pi G\rho}{3} - \frac{H_0^2}{a^2}(\Omega_0 - 1) \tag{110}$$

Diving by H_0^2 all through, we have

$$\begin{aligned}
 \frac{H^2}{H_0^2} &= \frac{8\pi G\rho}{3H_0^2} - \frac{1}{a^2}(\Omega_0 - 1) \\
 \frac{H^2}{H_0^2} &= \frac{\rho}{\rho_{c,0}} - \frac{(\Omega_0 - 1)}{a^2}
 \end{aligned} \tag{111}$$

The density parameters as of today can be written as

$$\begin{aligned}
 \Omega_{m,0} &= \frac{\rho_{m,0}}{\rho_{c,0}} \\
 \Omega_{r,0} &= \frac{\rho_{r,0}}{\rho_{c,0}} \\
 \Omega_{\Lambda,0} &= \frac{\rho_{\Lambda,0}}{\rho_{c,0}}
 \end{aligned} \tag{112}$$

The first Friedman equation becomes

$$\frac{H^2}{H_0^2} = \frac{\Omega_{m,0}}{a^3} + \frac{\Omega_{r,0}}{a^4} + \Omega_{\Lambda,0} + \frac{(\Omega_0 - 1)}{a^2} \tag{113}$$

Equation (113) can be written in the form

$$\frac{\dot{a}^2}{a^2 H_0^2} = \frac{\Omega_{m,0}}{a^3} + \frac{\Omega_{r,0}}{a^4} + \Omega_{\Lambda,0} + \frac{(\Omega_0 - 1)}{a^2} \tag{114}$$

$$\frac{\dot{a}^2}{H_0^2} = \frac{\Omega_{m,0}}{a} + \frac{\Omega_{r,0}}{a^2} + a^2\Omega_{\Lambda,0} + \Omega_0 - 1 \quad (115)$$

$$H_0 t = \int_0^a \frac{da}{\left(\frac{\Omega_{m,0}}{a} + \frac{\Omega_{r,0}}{a^2} + a^2\Omega_{\Lambda,0} + \Omega_0 - 1\right)^{\frac{1}{2}}} \quad (116)$$

Also, using the relation $\frac{\dot{a}}{a} = H$, we can differentiate H with rest to time as follows

$$\begin{aligned} \frac{d}{dt} \left(\frac{\dot{a}}{a} \right) \\ \frac{d}{dt} H = \frac{\ddot{a}}{a} - \frac{\dot{a}^2}{a^2} \\ \dot{H} = \frac{\ddot{a}}{a} - H^2 \end{aligned} \quad (117)$$

Therefore,

$$\frac{\ddot{a}}{a} = \dot{H} + H^2 \quad (118)$$

Using equation (118) in equation (88), we have,

$$\dot{H} + H^2 = -\frac{4\pi G}{3}(\rho + 3p) + \frac{\Lambda}{3} \quad (119)$$

Using equation (86) in (119),

$$\dot{H} + \frac{8\pi G\rho}{3} - \frac{k}{a^2} + \frac{\Lambda}{3} = -\frac{4\pi G}{3}(\rho + 3p) + \frac{\Lambda}{3} \quad (120)$$

We can let

$$P = \omega\rho \quad (121)$$

where, ω is called equation of state.

Therefore, substituting P equation (120) we have

$$\dot{H} + \frac{8\pi G\rho}{3} - \frac{k}{a^2} = -\frac{4\pi G}{3}\rho(1 + 3\omega) \quad (122)$$

$$\dot{H} = -4\pi G\rho - 4\pi G\omega\rho + \frac{k}{a^2} \quad (123)$$

$$\dot{H} = -4\pi G\rho(1 + \omega) + \frac{k}{a^2} \quad (124)$$

4.2.4 Dynamical Equations

Now we have obtained the three coupled equations

$$\dot{H} = -4\pi G\rho(1 + \omega) + \frac{k}{a^2} \quad (125)$$

$$\dot{a} = \left(\frac{8\pi G\rho a^2}{3} - k + \frac{\Lambda a^2}{3} \right)^{\frac{1}{2}} \quad (126)$$

$$\dot{\rho} = -3H\rho(1 + \omega) \quad (127)$$

These equations are evolution equations of Hubble parameter, scale factor and density of the universe respectively.

We rewrite them as differential equations as follows.

$$\frac{da}{dt} = \left(\frac{8\pi G\rho a^2}{3} - k + \frac{\Lambda a^2}{3} \right)^{\frac{1}{2}} \quad (128)$$

$$\frac{dH}{dt} = -4\pi G\rho(1 + \omega) + \frac{k}{a^2} \quad (129)$$

$$\frac{d\rho}{dt} = -3H\rho(1 + \omega) \quad (130)$$

Equations (128), (129) and (130) can be transformed as derivatives of h and Ω with respect to scale factor.

$$1 = \frac{8\pi G\rho}{3H^2} - \frac{k}{a^2 H^2} + \frac{\Lambda}{3H^2} \quad (131)$$

Taking $\frac{H}{H_0} = h$ we have

$$1 = \frac{\Omega_m}{h^2} + \frac{\Omega_k}{h^2} + \frac{\Omega_\Lambda}{h^2} \quad (132)$$

$$\frac{dH}{da} = \frac{-3H}{2a} \Omega(1 + \omega) - \frac{H}{a} \Omega_k \quad (133)$$

And can be written in terms of dimensionless Hubble parameter as

$$\frac{dh}{da} = \frac{-3h}{2a} \Omega(1 + \omega) - \frac{h}{a} \Omega_k \quad (134)$$

And

$$\frac{d\Omega}{ad\eta} = -\frac{2\Omega(1 + \omega)}{H} \frac{dH}{ad\eta} - 3H\Omega(1 + \omega)$$

$$\frac{d\Omega}{da} = -\frac{2\Omega(1+\omega)}{H} \frac{dH}{da} - \frac{3}{a}\Omega(1+\omega)$$

$$\frac{d\Omega}{da} = \frac{3}{a}\Omega^2(1+\omega) + \frac{2}{a}\Omega_k\Omega(1+\omega) - \frac{3}{a}\Omega(1+\omega) \quad (135)$$

The equations (132), (133) and (135) are the evolution background equations in general form.

4.2.4.1 Numerical solutions

We consider matter dominated universe where $w=0$

4.2.4.1.1 EdS model

$\Omega_m = 1$ and $\Omega_k = 0$

Background equations

$$\frac{dh}{da} = \frac{-3h}{2a} \quad (136)$$

$$\frac{d\Omega}{da} = 0 \quad (137)$$

Initial conditions

We consider initial conditions at decoupling. At decoupling, the scale factor corresponds with a redshift of 1000. The relation of redshift with scale factor is given by

$$a_{in} = \frac{1}{1+z} = \frac{1}{1001} = 10^{-3} \quad (138)$$

$$\begin{aligned}
a_{in} &= 10^{-3} \\
\Omega_{min} &= 1 \\
h_{in} &= a_{in}^{\frac{-3}{2}}
\end{aligned}
\tag{139}$$

4.2.4.1.2 Λ CDM model

$$\Omega_k = 0$$

The background equations are,

$$\frac{dh}{da} = \frac{-3h}{2a} \Omega \tag{140}$$

$$\frac{d\Omega}{da} = \frac{3}{a} \Omega^2 - \frac{3}{a} \Omega \tag{141}$$

Initial conditions

$$\begin{aligned}
a_{in} &= 10^{-3} \\
h_{in} &= (\Omega_m a_{in} + 1 - \Omega_\Lambda)^{\frac{1}{2}} \\
\Omega_{min} &= \frac{\Omega_{m0}}{h^2 a_{in}^3}
\end{aligned}
\tag{142}$$

4.2.4.1.3 Closed model

The background equations are,

$$\frac{dh}{da} = \frac{-3h}{2a} \Omega - \frac{h}{a} \Omega_k \tag{143}$$

$$\frac{d\Omega}{da} = \frac{3}{a}\Omega^2 + \frac{2}{a}\Omega_k\Omega - \frac{3}{a}\Omega \quad (144)$$

Initial conditions

$$a_{in} = 10^{-3} \quad (145)$$

$$h_{in} = (\Omega_m a_{in} + 1 - \Omega_\Lambda)^{\frac{1}{2}}$$

$$\Omega_{in} = \frac{\Omega_{m0}}{h^2 a_{in}^3} + \frac{\Omega_{k0}}{h^2 a_{in}^2}$$

CHAPTER FIVE: RESULTS AND DISCUSSION

In this chapter, we present the results and discussion of this research work. The results are obtained from numerical solutions of the coupled differential equations of Hubble parameter and density parameter as functions of the scale factor. We present results of Einstein de Sitter model, the standard cosmological model (Λ CDM) and the closed model of the universe and then compare them.

A graph of Hubble parameter and density parameter as functions of the scale factor in EdS model

The Einstein de Sitter is the simplest model of the universe where curvature and cosmological constants are taken to be zero.

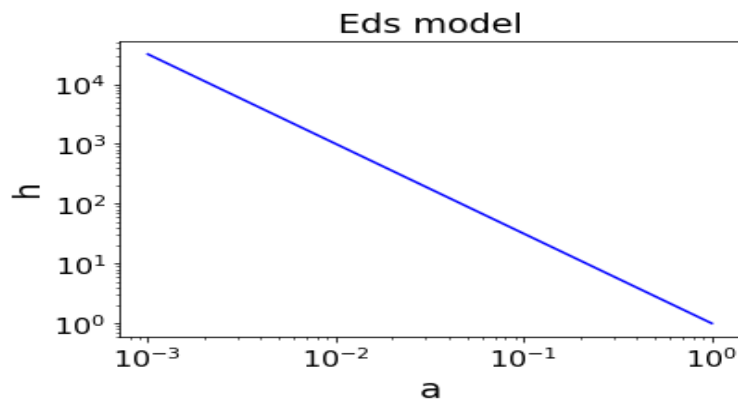


Figure 6. 1: A graph of h as a function of the scale factor

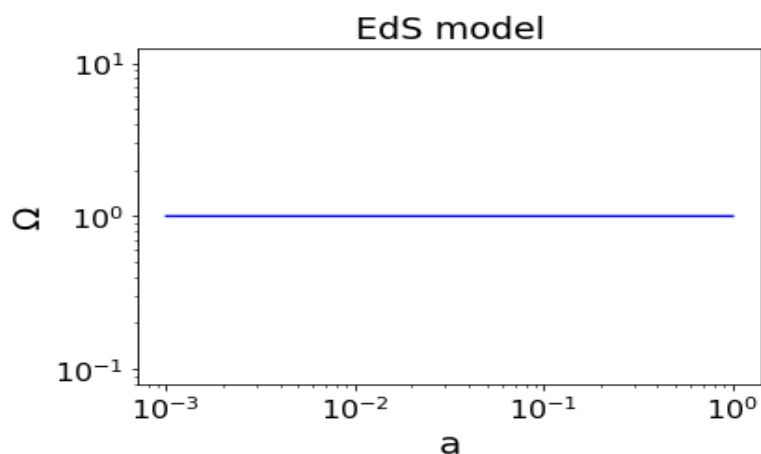


Figure 6. 2: A graph of a density parameter against scale factor.

From figure 6.1, the dimensionless Hubble parameter in the Einstein de Sitter model decreases uniformly with increase in scale. Figure 6.2 shows a graph of density parameter

against the scale factor. The value of density parameter remains constant as the scale factor increases until today. This is because, the system matter in the Einstein de Sitter model is assumed to be at rest.

A graph of Hubble parameter and density parameter as functions of the scale factor in Λ CDM model

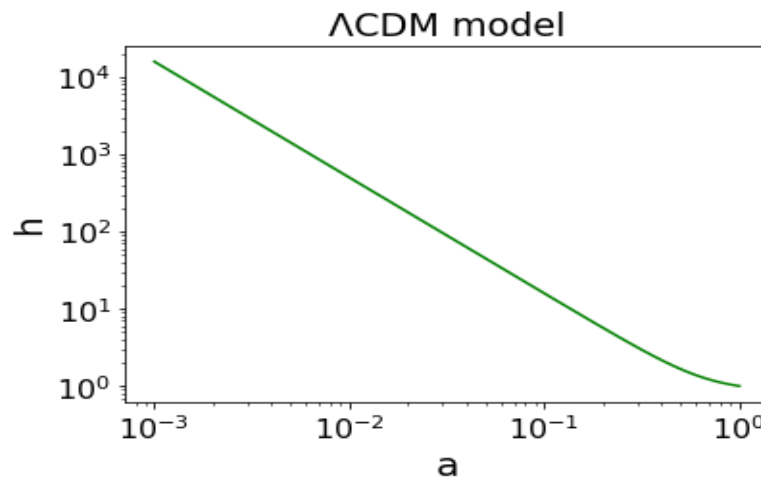


Figure 6. 3: A graph of h as a function of the scale factor for Λ CDM model.

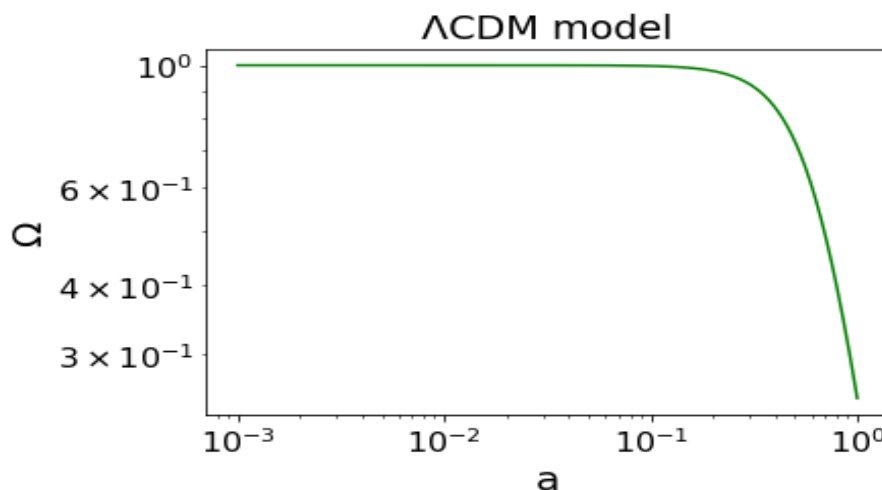


Figure 6. 4: A graph of density parameter for Λ CDM against the scale factor.

Figure 6.3 shows a graph of Hubble parameter with respect to the scale factor. From decoupling, the Hubble parameter decreases uniformly with increase in scale factor until the dark energy becomes dominant. Figure 6.4 shows a graph of density parameter as a function

of the scale factor. The value of density parameter at decoupling, where matter is dominant is one and it remains constant until dark energy dominates where its value reduces exponentially as the scale factor increases. Its value today is about 0.25.

A graph of Hubble parameter and density parameter as functions of the scale factor in Closed Model

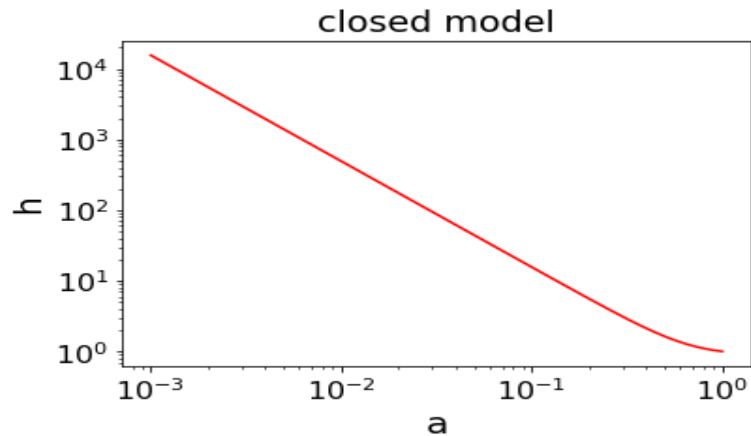


Figure 6. 5: A graph of h against scale factor (a) in closed model.

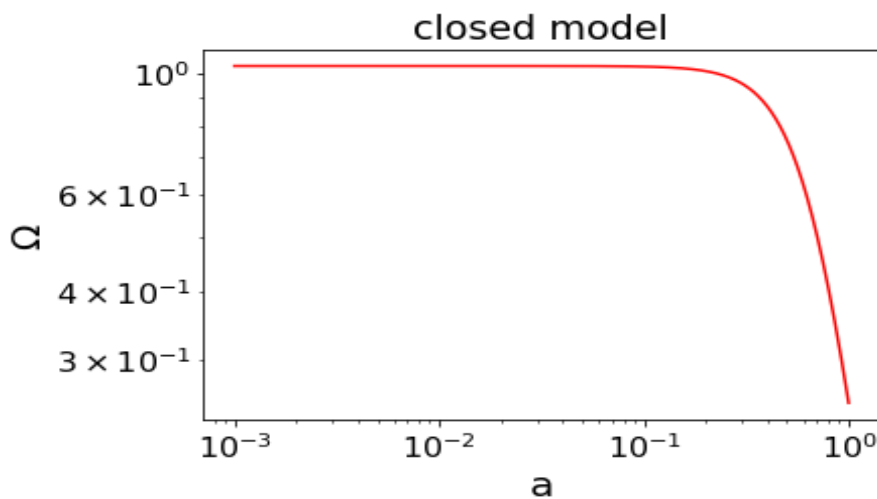


Figure 6. 6: A graph of density parameter with respect to scale factor for a closed universe
 Figure 6.5 is a graph of dimensionless Hubble parameter as a function of the scale factor. The Hubble parameter decreases uniformly from decoupling until the dark energy dominates.
 Figure 6.6 is a graph showing a relationship between density parameter and the scale factor. At decoupling, the density parameter of a closed universe model is slightly greater than one. This value remains constant as the scale factor increases. It then starts to reduce exponentially at some redshift. This is because; the dark energy starts to dominate over the matter of the universe.

Comparison of Hubble parameter graphs as a function of scale factor.

We present the comparison of change in the Hubble parameter with change in scale factor in the three cases.

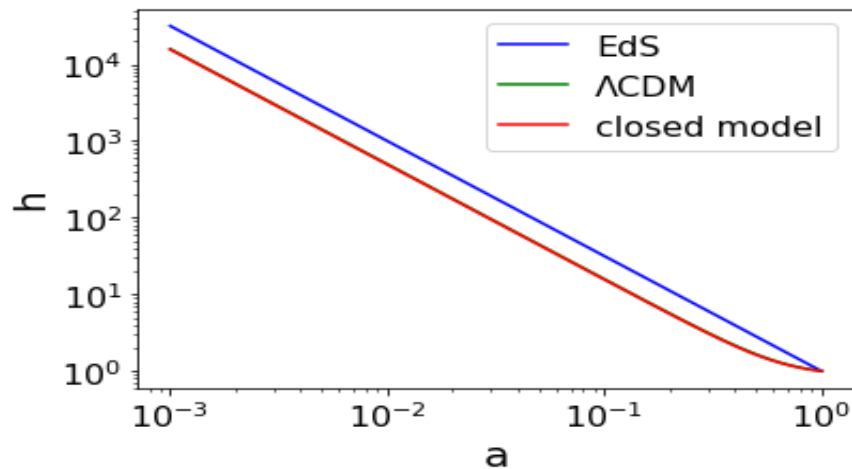


Figure 6. 7: Comparing the graphs of dimensionless Hubble parameter in EdS, Λ CDM and closed models

Figure 6.7 shows graphs of dimensionless Hubble parameter as function of the scale factor. From the graphs, we see that at decoupling the value of h in EdS model is greater than that of Λ CDM and closed models. However, the value of Hubble parameter decreases with increase in scale factor and converges at the scale factor today. In both Λ CDM and closed models, Hubble parameter exhibits the same trend until today.

Comparison of density parameter graphs as a function of scale factor.

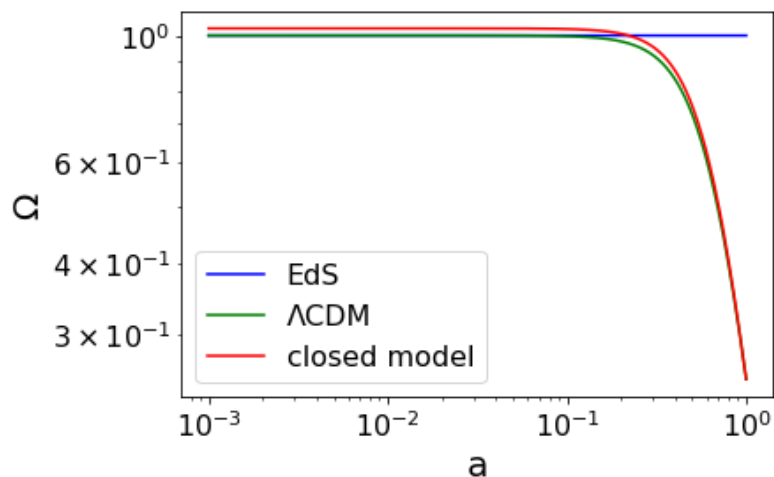


Figure 6. 8: Comparing the graphs of density parameter as a function of the scale factor in EdS, Λ CDM and closed models

Figure 6.8 shows graphs of density parameters as a function of the scale factor. From the graphs, the density parameters in EdS and Λ CDM are equal to one. The density parameter for a closed model is slightly greater than one. This shows that the closed universe contains more matter density which is greater than the critical density. The density parameter in EdS model remains constant while that of Λ CDM and closed models remains constant but at certain redshift, starts to decrease exponentially. This is due dominance of dark energy over the matter. The density parameter in both Λ CDM and closed universe converges to the same value at the scale factor today.

CHAPTER SIX: CONCLUSION AND RECOMMENDATION

This research was motivated by Di Valentino report on the evidence of a closed universe based on Planck's 2018 data that showed enhanced amplitude of CMB radiations. We explored this claims and modeled a shape of closed universe. To model this shape, a homogeneous and isotropic matter dominated (dust) universe was considered. Starting with Einstein Field equations and using Robertson-Walker-Lemaitre model we derived Friedmann equations and the equation of continuity of a perfect fluid. We obtained three coupled differential equations, on transforming them reduced to two background equations. By considering matter dominated universe at decoupling where $w=0$, we solved the equations numerically and plotted graphs of evolution of dimensionless Hubble parameter, and density parameter as the functions of the scale factor. We have presented the results of the three models starting with the simplest model; Einstein de Sitter model then Λ CDM model and lastly the closed model. From the results, we see that, for EdS model, the Hubble parameter reduces uniformly as the scale factor increases. Its density parameter remains constant. For the case of Λ CDM and closed universe, the Hubble parameter reduces uniformly until later when dark matter becomes dominant. There density parameters remain constant and when dark energy dominates, they start to reduce exponentially with increase in the scale factor. At decoupling, the density parameter of the closed universe is slightly greater than one. This means, the closed universe, its matter density is greater than critical density, thus closed universe contains enough matter to stop its expansion. We conclude that, it's this matter that contributed to the presence of enhanced lensing amplitude in CMB power spectra in PL18 report. This matter can cause deceleration of the universe. The deceleration implies that the universe will not expand forever and that at some point it will collapse. Since the Planck spectra from Planck's 2018 prefer a closed universe, although anomalies might have risen from undetected systematics or statistical fluctuations, we recommend that more observations to be carried out to ascertain whether there is a possible paradigm shift in cosmology and to whether new physics is required.

References

- Ade P.A.R, e. a. (2016). *Planck 2015 results. XIII> Cosmological Parameters*. Planck Collaboration.
- Amandola. (2021). *Lecture Notes:Cosmology*. University of Heidelberg.
- Balbi A. (2004). *CMB and precision cosmology: status and Prospects*. Italy, Roma: Università di Roma.
- Che-Qiu I, e. a. (2019). *Towards to H_0 Tensin by the Theoretical hubble Parameter in the Infite Future*. Beijing Normal University.
- Di Valentino E, e. a. (2019). *Planck evidence for a Closed Universe and possible Crisis*. Universita di Roma.
- Heinesen , A., & Buchert , T. (2020). Solving the curvature and Hubble parameter.
- Jun-Qing. (2013). *Dark energy Constraints After Plank*. Institute of Hihg Energy Physics.
- Kolb E. W, e. a. (1989). *The Early Universe*. Addison-Wesley.
- Longair S. (2004). *A Brief History of Cosmology*. Cambridge, UK: Cavendish Laboratory.
- Peacock. (1999). *Cosmological Physics*. Cambridge Unioversity Press.
- Piattela. (2018). *Lecture Notes in Comology*. University Federal do Esirito Santo.
- Robson B. (2019). *Standard Model of Cosmology*. Canberra, Australia: The Australian National University.
- Scott. (2003). *Modern Cosmology*. San Diego: Academic Press.
- Shu W. (2015). *The Geometry of the Universe*. Taiwan: National Tsing Hua University.